Animal Nutrition 16 (2024) 158–173

Contents lists available at ScienceDirect

Animal Nutrition

journal homepage: http://www.keaipublishing.com/en/journals/aninu/

Original Research Article

Leucine regulates lipid metabolism in adipose tissue through adipokine-mTOR-SIRT1 signaling pathway and bile acid–microbe axis in a finishing pig model

Yunju Yin [a, b], Saiming Gong [a, b], Mengmeng Han [a, c], Jingzun Wang [d], Hanjing Shi [a, e], Xianji Jiang [a, b], Liu Guo [a, c], Yehui Duan [a], Qiuping Guo [a], Qinghua Chen [b], Fengna Li [a, c, *]

[a] Key Laboratory of Agro-ecological Processes in Subtropical Region, Institute of Subtropical Agriculture, Chinese Academy of Sciences, Hunan Provincial Key Laboratory of Animal Nutritional Physiology and Metabolic Process, Hunan Provincial Engineering Research Center for Healthy Livestock and Poultry Production, Changsha 410125, China
[b] College of Animal Science and Technology, Hunan Agricultural University, Changsha 410128, China
[c] College of Modern Agricultural Sciences, University of Chinese Academy of Sciences, Beijing 100049, China
[d] College of Life Science and Engineering, Northwest Minzu University, Lanzhou 730124, China
[e] College of Life Sciences, Hunan Normal University, Changsha 410128, China

ARTICLE INFO

Article history:
Received 28 November 2022
Received in revised form
7 October 2023
Accepted 12 October 2023
Available online 16 November 2023

Keywords:
Leu
Lipid metabolism
Gut microbiota
Bile acid

ABSTRACT

This study was conducted to explore the regulatory mechanism of leucine (Leu) on lipid metabolism of finishing pigs. Twenty-four Duroc × Landrace × Large cross pigs with an average body weight of 68.33 ± 0.97 kg were randomly allocated into 3 treatment groups with 8 replicates per group (1 pig per replicate). The dietary treatments were as follows: control group (CON), 0.25% Leu group and 0.50% Leu group. The experimental period was 42 d. The results showed as follows. (1) Compared with the CON, 0.25% and 0.50% Leu increased ($P < 0.01$) the average daily gain (ADG), while the average backfat thickness (ABT) and the ratio of feed intake to body weight gain (F:G ratio) were decreased ($P < 0.05$). (2) In the 0.25% Leu group, the relative mRNA expression levels of sterol regulatory element binding protein-1c (*SREBP1c*), recombinant fatty acid transport protein 1 (*FATP1*), chemerin and peroxisome proliferator-activated receptor γ (*PPARγ*) were decreased but the level of fatty acid binding protein 4 (*FABP4*) and fatty acid translocase (*FAT/CD36*) were increased in backfat tissue. In the 0.25% Leu group, the protein levels of p-Rictor, p-Raptor, p-eIF4E-binding protein 1 (p-4EBP1), p-silent mating type information regulator 2 homolog 1 (p-SIRT1) and acetylation ribosome s6 protein kinase 1 (Ac–S6K1) were increased ($P < 0.05$). (3) Compared to the CON, the diversity of gut microbiota in the 0.25% Leu group was increased. Principal component analysis showed that the relative abundance of Bacteroidetes, *Lactobacillus* and *Desulfovibrio* was higher in the 0.25% Leu group than the CON, but the relative abundance of Firmicutes, *Treponema* and *Shigella* was lower than in the CON ($P < 0.05$). (4) Four different metabolites were screened out from the serum of finishing pigs including allolithocholic acid (alloLCA), isolithocholic acid (isoLCA), ursodeoxycholic acid (UDCA) and hyodeoxycholic acid (HDCA), which correlate to various degrees with the above microorganisms. In conclusion, Leu could promote adipose tissue lipolysis of finishing pigs through the mTOR-SIRT1 signaling pathway, and S6K1 is acetylated at the same time, and the interaction between gut microbiota and bile acid metabolism is also involved.

* Corresponding author.
E-mail address: lifengna@isa.ac.cn (F. Li).
Peer review under responsibility of Chinese Association of Animal Science and Veterinary Medicine.

Production and Hosting by Elsevier on behalf of KeAi

1. Introduction

Leucine (Leu), chemical name α-aminoisohexanoic acid, is an essential amino acid (Salles et al., 2017) which regulates protein metabolism and provides oxidative energy to the body (Anthony et al., 2000; Atherton et al., 2010). Leu dramatically increases

https://doi.org/10.1016/j.aninu.2023.10.005

leptin secretion in rat adipocytes via the mammalian target of rapamycin (mTOR) pathway (Roh et al., 2003), reduces hyperglycemia, cholesterol and fat deposition caused by a high-fat diet (HFD) (Zhang et al., 2007). Previous studies by our team have found that increasing the dietary Leu to branched-chain amino acid (BCAA) ratio can regulate the expression of silent mating type information regulator 2 homolog 1 (SIRT1) and reduce fat deposition in pigs (Duan et al., 2018). Previous studies have shown the interaction between SIRT1 and mTOR, SIRT1 inhibits the acetylation of ribosome s6 protein kinase 1 (S6K1) and the mTOR-dependent phosphorylation of S6K1 (Bianchi and Giovannini, 2018). Bile acids (BA) interact with gut microbes and both are involved in lipid metabolism (Staley et al., 2017). The Leu metabolite β-hydroxy-β-methyl butyrate (HMB) is known to mediate lipid metabolism by improving microbial diversity (He et al., 2018). However, researches on the role of Leu regulating the lipid metabolism of finishing pigs are limited and the mechanism is not clear. Therefore, based on the scientific hypothesis that Leu promotes adipose tissue lipid metabolism through the adipokine-mTOR-SIRT1 signaling pathway and the BA-microbiota axis, we investigated the regulatory effect of adipose tissue lipid metabolism by Leu using a finishing pig model and revealed the relationship between mTOR and SIRT1 proteins and their key roles in the process. We aimed to provide a theoretical basis and new ideas for the scientific application of Leu to improve pig carcass quality and expand on the nutritional theory of functional amino acid regulation of lipid metabolism.

2. Materials and methods

2.1. Animal ethics statement

This animal experiment was permitted by the Animal Care and Use Committee of Institute of Subtropical Agriculture, Chinese Academy of Sciences, Changsha, China under permit No. ISA-2021-015. It conformed to the requirements of animal ethics and animal welfare. It complied with the ARRIVE guidelines.

2.2. Animals and experimental design

Twenty-four healthy finishing pigs (Duroc × Landrace × Large) with a body weight of 68.33 ± 0.97 kg were randomly allocated into three groups according to body weight, with 8 replicates per group (1 pig per replicate). The formal trial was started after a 3-d adaptive feeding trial. Each pig was fed in a single pen. The experimental diet was a corn-soybean meal basal diet meeting NRC (2012) standards with a crude protein level of approximately 14%. The first 4 limiting amino acids (Lys, Met, Trp, Thr) were consistent in each group, and leucine was only added in the experimental group. The ingredients and nutritional composition of the basal diets are shown in Table 1. Crude protein (CP) in diets was determined by Kjeldahl method (China National Standard, 2018), and Ca and P content was determined by atomic emission spectrometry (Ministry of Agriculture of the People's Republic of China, 2018). Experimental diets were as follows: (1) basal diet; (2) basal diet + 0.25% Leu; (3) basal diet + 0.50% Leu. The experiment lasted 42 d and was slaughtered at 190 d of age.

2.3. Sample collection

All pigs were fasted overnight (12 h) at the end of the trial and slaughtered by bleeding. Blood samples were placed in plain tubes at room temperature for 30 min before slaughter and then centrifuged at 3000 × *g*, 4 °C for 10 min. The supernatant was aspirated in an Eppendorf (EP) tube and stored at −80 °C for testing. The perirenal fat and backfat samples were immediately removed and stored at −20 °C to determine chemical composition or placed in liquid N_2, then stored at −80 °C for the quantitative real-time polymerase chain reaction (PCR) analysis. Fresh backfat samples (1 cm^3) were fixed with paraformaldehyde fixative, paraffin sectioned, and stained with hematoxylin and eosin. Colonic digesta was collected and stored at −80 °C for 16S rRNA sequencing.

Table 1
Ingredients and nutritional composition of basal diets (low protein diet) (% fresh sample basis).

Item	Leucine levels, %		
	0	0.25	0.50
Ingredients			
Corn	79.42	80.00	80.36
Soybean meal	14.80	13.88	13.20
Wheat bran	3.00	3.00	3.00
Lysine	0.28	0.30	0.32
Methionine	0.00	0.01	0.02
Threonine	0.07	0.08	0.09
Tryptophan	0.01	0.02	0.02
Leucine	0.00	0.25	0.50
Isoleucine	0.00	0.02	0.02
Valine	0.00	0.01	0.03
$CaHPO_4$	0.60	0.60	0.60
Limestone	0.52	0.53	0.54
Salt	0.30	0.30	0.30
Premix[1]	1.00	1.00	1.00
Total	100.00	100.00	100.00
Nutrient content			
ME[2], MJ/kg	12.73	12.70	12.66
Crude protein	13.58	13.69	13.88
SID Lysine[2]	0.74	0.73	0.73
SID (Methionine + Cysteine)	0.42	0.42	0.42
SID Threonine	0.47	0.47	0.47
SID Tryptophan	0.13	0.14	0.13
SID Leucine	1.12	1.34	1.57
Total Ca	0.51	0.46	0.48
Total P	0.59	0.50	0.56

ME = metabolizable energy; SID = standardized ileal digestibility.
[1] Supplied per kilogram of diet: vitamin A, 15,000 IU; vitamin D_3, 3000 IU; vitamin E, 40 IU; vitamin K_3, 4 mg; vitamin B_1, 3 mg; vitamin B_2, 10 mg; vitamin B_6, 4 mg; vitamin B_{12}, 0.03 mg; biotin, 0.2 mg; folic acid, 2 mg; niacin, 35 mg; D-calcium pantothenate, 20 mg; Cu (as copper sulfate), 15 mg; Fe (as ferrous sulfate), 80 mg; Mn (as manganese oxide), 15 mg; Zn (as zinc oxide), 70 mg; I (as potassium iodide), 0.5 mg; and Se (as sodium selenite), 0.3 mg.
[2] Calculated values for ME and SID amino acids.

2.4. Carcass traits analysis

After slaughter, the carcass was weighed on the left side and the slaughter rate was calculated. Average backfat thickness (the 3rd to 4th lumbar vertebra, the 10th to 11th lumbar vertebra and the last rib) and the loin-eye area were measured from the left side of the carcass.

2.5. Serum biochemical indicator measurements

Total protein (TP), glucose (GLU), cholesterol (CHOL), triglyceride (TG), very low-density lipoprotein cholesterol (VLDL-C), blood urea nitrogen (BUN), low-density lipoprotein cholesterol (LDL-C), albumin (ALB) and high-density lipoprotein cholesterol (HDL-C) in serum was determined by a Cobas C311 Analyser (Roche Diagnostics, Basal, Switzerland) and manufacturer-specified commercial kits (Leadman Biotech Limited, Beijing, China).

2.6. Serum cytokine measurements

Insulin-like growth factor 1 (IGF1), myostatin (MSTN), fibroblast growth factor 21 (FGF21), leptin, insulin (INS), interleukin 6 (IL-6),

chemerin and adiponectin in serum were detected by ELISA kits (Changsha Aoji Biotechnology Co., Ltd, Changsha, China).

2.7. Measurement of key enzyme activity

ELISA kits (Changsha Aoji Biotechnology Co., Ltd, Changsha, China) were used to determine the activity of acyl-CoA cholesterol acyltransferase (ACAT), hormone-sensitive lipase (HSL), adipose triacylglyceride lipase (ATGL), fatty acid synthase (FAS), acetyl-CoA carboxylase (ACC) and lipoprotein lipase (LPL) in backfat and perirenal fat tissue samples.

2.8. Determination of medium-long chain fatty acids in backfat tissue

The freeze-dried backfat samples were ground and weighed to about 0.5 g, transferred to a 50-mL centrifuge tube with 4 mL benzene-petroleum ether (1:1) mixed solvent, and extracted in a closed manner for 24 h. Then 4 mL potassium hydroxide methanol solution (0.4 mol/L) was added to the mixture, which was shaken in a vortex mixer for 3 min and left to stand for 30 min. After adding ultra-pure water to the centrifuge tube for stratification, the upper solution was taken and 5 g anhydrous sodium sulfate added to absorb the water in the sample. A 200-μL sample was then added to 800 μL hexane and diluted with a 0.22-μm filter before sampling. Chromatographic condition is the following. Column SP-2560: 100 m × 0.25 mm × 0.2 μm; carrier gas: high pure nitrogen, flow rate 0.8 mL/min; injection volume: 1 μL, split ratio 20:1; flame ionization detector: temperature 280 °C, hydrogen 30 m/min, and air 400 mL/min; column temperature: the initial temperature was kept at 140 °C for 5 min, then heated to 220 °C at 3 °C/min, then maintained for 40 min.

2.9. Histological analysis of backfat tissue

The mean cross-sectional area and number of adipocytes in the backfat tissue were determined by classical hematoxylin and eosin staining. Four μm tissue sections were cut continuously with a paraffin microtome (RM, 2016; Leica Instruments Co., Ltd, Shanghai, China). Slices were stained by hematoxylin dye solution for 3 to 5 min, rinsed with tap water, then dehydrated with 85% and 95% gradient alcohol for 5 min, respectively, then stained with eosin dye solution for 5 min, dehydrated by anhydrous ethanol, and finally sealed with neutral glue. Scanning of slices was performed with the panoramic slice scanner of Pannoramic Desk/MIDI/250/1000 (3DHISTECH, Hungary). The scanned slice was opened with CaseViewer (3 DHISTECH, Hungary) and the field of view was intercepted for calculation and analysis using Image Pro Plus 6.0 (Media Cybernetics, Maryland, USA).

2.10. Total RNA isolation and quantitative real-time PCR analysis

Total RNA was extracted from backfat and perirenal fat samples with Trizol reagent (Hunan Aikerui Bioengineering Co., Ltd, Changsha, China). Determination of RNA concentration and purity was performed by NanoDrop ND2000 (NanoDrop Technologies Inc., Wilmington, DE) after extraction, and samples with OD260/280 between 1.8 and 2.2 were qualified. The RNA concentration of all samples was adjusted to 1000 ng/μL and then reverse transcribed into cDNA with Evo M-MLV Reverse Transcription Kit (Hunan Aikerui Bioengineering Co., Ltd, Changsha, China). SYBR Green Premix Pro Taq HS qPCR Kits (Hunan Aikerui Bioengineering Co., Ltd, Changsha, China) and an ABI 7900 HT real-time PCR system (Applied Biosystems, Branchburg, NJ) were used for quantitative real-time PCR. A total volume of 10 μL PCR solution consisted of 2 μL cDNA, 2.2 μL RNase free water, 5 μL SYBR Green Pro Taq HS premix and 0.4 μL primer pairs. The program for the qPCR instrument consisted of 95 °C for 30 s for 1 cycle, 95 °C for 5 s for 40 cycles, and 60 °C for 30 s. The relative expression of mRNA of each gene was calculated by the $2^{-\Delta\Delta Ct}$ method ($\Delta\Delta Ct = \Delta Ct_{\text{target gene}} - \Delta Ct_{\text{GAPDH}}$) with glyceraldehyde-3-phosphate dehydrogenase (*GAPDH*) as the endogenous control gene. Sequences of primers are shown in Table 2.

2.11. Western blotting analysis

An appropriate amount of back adipose tissue samples were weighed and added into radioimmunoprecipitation assay buffer (RIPA) lysate for ice solubilization. The protein concentration was determined used a BCA protein assay kit (Beyotime biotechnology, Shanghai, China). Sodium dodecyl sulfate polyacrylamide gel electrophoresis (SDS-PAGE) was then conducted. First, the glass

Table 2
Primers used for quantitative real-time PCR.

Genes[1]	Primers	Sequences (5′ to 3′)	Product size, bp
ACC	Forward	ACCGAATTGGTTCCTTTGGAC	169
	Reverse	CCAGTCCGATTCTTGCTCCA	
ATGL	Forward	TCACCAACACCAGCATCCA	95
	Reverse	GCACATCTCTCGAAGCACCA	
HSL	Forward	CCCATCCTCTCCATCGACT	167
	Reverse	CAGCAGTAGGCGTAGAAGCAC	
LPL	Forward	CTCGTGCTCAGATGCCCTAC	148
	Reverse	GGCAGGGTGAAAGGGATGTT	
FAS	Forward	CTACCTTGTGGATCACTGCATAGA	114
	Reverse	GGCGTCTCCTCCAAGTTCTG	
PPAR γ	Forward	GTGGAGACCGCCCAGGTTTG	124
	Reverse	GGGAGGACTCTGGGTGGTTCA	
SREBP-1c	Forward	CTGCTTGAGCTTCTGGTTGC	218
	Reverse	GCTACCGCTCCTCCATCAAT	
FATP1	Forward	ACCACTCCTACCGCATGCAG	78
	Reverse	CCACGATGTTCCCTGCCGAGT	
FAT/CD36	Forward	TGTGGATACTTGGAGGTGGG	160
	Reverse	TGCTGGTTGGAATACAGTGG	
FABP4	Forward	GAAAGTCAAGAGCACGATAACC	227
	Reverse	CAAGATACATTCCACCACCAAC	
C/EBPα	Forward	GCAGAGATCCCTATAAACCAGC	84
	Reverse	TTCAAAGCCCCAAGTCCC	
Adiponectin	Forward	CAAGAAACCACCGAGAAGC	563
	Reverse	TCCAGATAGAGGAGCACAGAG	
Chemerin	Forward	AGTTCCACAAGCACCCACCC	148
	Reverse	GCTTTCTTCCAGTCCCTCTT	
Leptin	Forward	CCGATTCCTGTGGCTTTGG	254
	Reverse	TGGAAGGCAGACTGGTGAGG	
Resistin	Forward	TCCCTCCTCTTCCTCCCAACC	440
	Reverse	ATTTCCAGCCCTGCCCCAC	
SIRT1	Forward	ACTCTCCCTCTTTTAGACCAAGC	149
	Reverse	AAACCTGGACTCTCCATCGG	
SIRT2	Forward	CTGTCACTACTTCATGCGCCTG	116
	Reverse	CCTCCACCAAGTCCTCCTGTT	
SIRT3	Forward	CACGTTTACAAACATGAACC	194
	Reverse	CATGCTAGATTGCCCTAGT	
SIRT4	Forward	CCCTGACCTTGTAGATGTCATTG	114
	Reverse	GTCACGATGATACAG-TTCTGCAAA	
SIRT5	Forward	ATGGCTCGTCCAAGTTCAAATATGGC	377
	Reverse	TGGATTTCCAGAAGGTTCTTGGTGC	
SIRT6	Forward	CAGTACGTCAGAGACACGGTTG	178
	Reverse	GTCCAGAATGGTGTCTCTCAGC	
GAPDH	Forward	ACTCACTCTTCTACCTTTGATGCT	123
	Reverse	TGTTGCTGTAGCCAAATTCA	

[1] *ACC* = acetyl CoA carboxylase; *ATGL* = adipose triacylglyceride lipase; *HSL* = hormone-sensitive lipase; *LPL* = lipoprotein lipase; *FAS* = fatty acid synthase; *PPARγ* = peroxisome proliferator-activated receptor γ; *SREBP-1c* = sterol regulatory element binding protein-1c; *FATP1* = fatty acid transport protein 1; *FAT/CD36* = fatty acid translocase; *FABP4* = fatty acid binding protein 4; *C/EBPα* = CCAAT enhancer-binding proteinsα; *SIRT1* = silent mating type information regulator 2 homolog 1; *GAPDH* = glyceraldehyde-3-phosphate dehydrogenase.

Table 3
Growth performance of finishing pigs fed the diets with various levels of leucine.

Item[1]	Leucine levels, %			*P*-value
	0	0.25	0.50	
Initial weight, kg	69.57 ± 2.01	67.76 ± 1.26	67.57 ± 1.87	0.67
Final weight, kg	88.70 ± 1.91	93.23 ± 1.60	91.58 ± 1.81	0.07
ADFI, kg/d	2.26 ± 0.07	2.46 ± 0.12	2.24 ± 0.16	0.55
ADG, kg/d	0.42 ± 0.03^{b}	0.61 ± 0.03^{a}	0.59 ± 0.04^{a}	<0.01
F:G ratio	3.95 ± 0.27^{a}	3.20 ± 0.15^{b}	3.17 ± 0.10^{b}	<0.01
ABT, mm	20.69 ± 1.60^{a}	16.34 ± 0.38^{b}	16.29 ± 0.73^{b}	0.01
Loin-eye area, cm^2	30.06 ± 0.89^{b}	34.30 ± 1.41^{ab}	36.22 ± 2.22^{a}	0.03
Lean mass percentage, %	59.78 ± 0.58	60.66 ± 0.59	61.07 ± 0.27	0.22
Total fat rate percentage, %	15.67 ± 0.95	14.00 ± 0.66	15.57 ± 0.24	0.21

$^{a, b}$ Within a row, means without a common superscript are significantly different ($P < 0.05$).
[1] ADG = average daily weight gain; F:G ratio = the ratio of feed intake to body weight gain; ABT = average backfat thickness.

plate was cleaned, and then the suitable concentration of glue was formulated according to the protein concentration of the sample. The loading volume was calculated and an equal volume of buffer and 1/10 volume of β-Mercaptoethanol were added and put into a Mastercycler Nexus PCR instrument (Eppendorff, Hamburg, Germany) and mixed well. The sample was added and electrophoresis performed, then transferred to a membrane and the primary and secondary antibodies were incubated for color development after sealing the membrane.

2.12. Sequencing of 16S rRNA gene amplicons

PCR amplification of the V3–V4 region of the bacterial 16S rRNA gene was performed with forward primer 338F (5′-ACTCCTACGGGAGGCAGCA-3′) and reverse primer 806R (5′-GGACTACHVGGGTWTCTAAT-3′). Sample-specific 7 bp barcodes were combined into primers for multiple sequencing. The components of PCR were 5 μL of buffer (5×), 0.25 μL of FastPfu DNA Polymerase (5 U/μL), 2 μL (2.5 mol/L) of dNTPs, 1 μL (10 μmol/L) each of forward and reverse primers, 14.75 μL of ddH_2O, and 1 μL of DNA template. Thermal cycling included an initial denaturation at 98 °C for 5 min, followed by 25 cycles consisting of 98 °C denaturation for 30 s, 53 °C annealing for 30 s, 72 °C extension for 45 s, and 72 °C final extension for 5 min. PCR amplicons were purified by using Vazyme VAHTSTM DNA Clean Beads (Vazyme, Nanjing, China) and quantified by the Quant-iT PicoGreen dsDNA Assay Kit (Invitrogen, Carlsbad, CA, USA). When individual quantification steps were completed, equal amounts of amplicons were pooled and sequenced at 2 × 250 bp at both ends using the Illlumina NovaSeq platform and NovaSeq 6000 SP kit (500 cycles) from Shanghai Personal Biotechnology Co. (Shanghai, China).

2.13. Bile acid targeting metabolomics

The proper amount of 39 kinds of bile acid standard products were weighed, and proper amount of mother liquor was taken to make mixed standard products. The working standard solution was made by diluting the mother liquor one to one with an appropriate concentration of methanol. Both the mother liquor and working standard solution were stored at −20 °C.

2.13.1. Metabolite extraction

Serum was transferred to a 2-mL EP tube and 600 μL of methanol (−20 °C) was added. The mixture was subject to 60 s of vortex shaking and 10 min of centrifugation at 13,400 × *g* at 4 °C. Following this, 400 μL of the supernatant was concentrated and dried and 100 μL redissolved in 30% methanol and swirled for 30 s. Then 50 μL of supernatant was added to 200 μL 30% methanol, swirled for 30 s, and 90 μL of supernatant was loaded into the test bottle for examination. The following formula was used: Sample content (μg/mL) = sample concentration (ng/mL) × 0.7 × 0.25 × 5/sample volume (μL) (Bhargava et al., 2020; Hu et al., 2020).

2.13.2. Chromatographic conditions

The chromatographic column (2.1 mm × 100 mm, 1.7 μm; ACQUITY UPLC BEH C18, Waters inc., USA) was used. The sample volume was 5 μL; the column temperature was 40 °C; and the mobile phases were 0.01% formic acid in water (A) and acetonitrile (B). Gradient elution conditions were 0 to 4 min, 25% B; 4 to 9 min, 25% to 30% B; 9 to 14 min, 30% to 36% B; 14 to 18 min, 36% to 38% B; 18 to 24 min, 38% to 50% B; 24 to 32 min, 50% to 75% B; 32 to 33 min,

Table 4
Effects of dietary leucine on serum biochemical indexes of finishing pigs.

Item[1]	Leucine levels, %			*P*-value
	0	0.25	0.50	
TP, g/L	79.33 ± 0.65	82.40 ± 0.31	82.74 ± 1.94	0.08
ALB, g/L	43.98 ± 1.04	44.15 ± 1.58	45.48 ± 1.47	0.71
BUN, mmol/L	3.14 ± 0.16^{a}	2.30 ± 0.18^{b}	2.60 ± 2.1^{b}	0.01
GLU, mmol/L	3.60 ± 0.19	3.08 ± 0.35	3.34 ± 0.4	0.51
TG, mmol/L	0.71 ± 0.07^{a}	0.48 ± 0.03^{b}	0.47 ± 0.02^{b}	<0.01
LDL-C, mmol/L	1.88 ± 0.12^{a}	1.45 ± 0.05^{b}	1.38 ± 0.11^{b}	<0.01
HDL-C, mmol/L	0.75 ± 0.08	0.80 ± 0.04	0.69 ± 0.23	0.38
VLDL-C, mmol/L	14.58 ± 0.12^{a}	12.50 ± 0.05^{b}	14.28 ± 0.11^{b}	0.03
CHOL, mmol/L	2.85 ± 0.15^{a}	2.29 ± 0.05^{b}	2.15 ± 0.11^{b}	<0.01

$^{a, b}$ Within a row, means without a common superscript are significantly different ($P < 0.05$).
[1] TP = total protein; ALB = albumin; BUN = blood urea nitrogen; Glu = glucose; CHOL = cholesterol; TG = triglyceride; HDL-C = high-density lipoprotein cholesterol; LDL-C = low-density lipoprotein cholesterol; VLDL-C = very low-density lipoprotein cholesterol.

Table 5
Effects of different levels of Leu on serum adipokine concentration of finishing pigs.

Item[1]	Leucine levels, %			*P*-value
	0	0.25	0.50	
INS, pg/mL	1.37 ± 0.04	1.37 ± 0.04	1.32 ± 0.04	0.61
IGF1, ng/mL	42.80 ± 2.32^{b}	53.60 ± 2.92^{a}	54.80 ± 1.60^{a}	<0.01
MSTN, pg/mL	4.32 ± 0.12^{b}	4.63 ± 0.09^{ab}	4.99 ± 0.19^{a}	<0.01
Chemerin, ng/mL	14.90 ± 0.88^{a}	11.73 ± 0.88^{b}	14.18 ± 0.92^{ab}	<0.01
FGF21, pg/mL	1.27 ± 0.02^{b}	1.54 ± 0.13^{a}	1.27 ± 0.02^{b}	0.04
Leptin, pg/mL	5.86 ± 0.12^{b}	6.41 ± 0.12^{a}	6.25 ± 0.17^{ab}	0.02
IL-6, pg/mL	0.58 ± 0.04^{b}	0.77 ± 0.03^{a}	0.75 ± 0.03^{a}	<0.01
Adiponectin, ng/mL	25.33 ± 0.91^{b}	27.84 ± 2.14^{b}	33.17 ± 1.74^{a}	0.01

$^{a, b}$ Within a row, means without a common superscript are significantly different ($P < 0.05$).
[1] IGF1 = insulin-like growth factor 1; MSTN = myostatin; FGF21 = fibroblast growth factor 21; INS = insulin; IL-6 = interleukin 6.

Table 6
Effects of different levels of leucine on key enzyme activities related lipid metabolism of finishing pigs.

Item[1]	Leucine levels, %			*P*-value
	0	0.25	0.50	
Backfat				
ACC, U/g	237.11 ± 8.55[a]	230.31 ± 5.57[a]	200.78 ± 6.85[b]	<0.01
HSL, U/g	7.03 ± 0.37[c]	11.48 ± 0.34[a]	9.29 ± 0.77[b]	<0.01
LPL, U/g	3.94 ± 0.25[b]	5.24 ± 0.23[a]	4.51 ± 0.23[b]	<0.01
ATGL, mIU/g	2381.66 ± 101.83	2471.45 ± 83.27	2451.14 ± 86.58	0.76
ACAT, U/g	0.70 ± 0.02[b]	0.95 ± 0.04[a]	0.89 ± 0.05[a]	<0.01
FAS, U/g	15.35 ± 0.84[a]	12.97 ± 0.72[b]	12.23 ± 0.72[b]	0.02
Perirenal fat				
ACC, U/g	311.59 ± 13.38	283.89 ± 14.44	276.08 ± 17.66	2.39
HSL, U/g	10.65 ± 0.40	11.97 ± 0.38	11.98 ± 0.66	0.10
LPL, U/g	4.64 ± 0.27[b]	6.15 ± 0.34[a]	5.72 ± 0.27[a]	<0.01
ATGL, mIU/g	2636.74 ± 49.36	2976.72 ± 140.98	2880.86 ± 120.11	0.10
ACAT, U/g	0.72 ± 0.04[b]	0.95 ± 0.04[a]	0.82 ± 0.07[ab]	0.01
FAS, U/g	16.21 ± 0.76	13.91 ± 0.70	14.56 ± 0.99	0.14

[a-c] Within a row, means without a common superscript are significantly different ($P < 0.05$).
[1] ACC = acetyl-CoA carboxylase; HSL = hormone-sensitive lipase; LPL = lipoprotein lipase; ATGL = adipose triacylglyceride lipase; ACAT = acyl-CoA cholesterol acyltransferase; FAS = fatty acid synthase.

75% to 90% B; 33 to 35.5 min, 90% to 25% B. The flow rate was 0.25 mL/min (Hu et al., 2020; Yang et al., 2017b).

2.14. Statistical analysis

The data from experiments were analyzed by one-way ANOVA (analysis of variance) with SPSS (version 26.0, SPSS Inc., Chicago, USA), followed by Duncan's multiple comparison test. Results were shown as mean ± SEM, with $P < 0.05$ considered significant and $0.05 \leq P < 0.10$ as a trend. The raw metabolomics data were converted to mzXML format by ProteoWizard, processed using a proprietary R program package (kernel XCMS), and matched with a self-built secondary mass spectrometry database for substance annotation, with the algorithm scoring Cutoff value set to 0.3. The data were then imported into SIMCA 14.1 software (MKS Data Analytics Solutions, Umea, Sweden) for multivariate statistical analysis and differential metabolite screening.

3. Results

3.1. Growth performance and carcass traits

The effects of Leu on growth performance and carcass traits of finishing pigs are shown in Table 3. No significant differences in final weight, lean mass percentage and total fat rate percentage were found among the three groups ($P > 0.05$), but the average daily gain (ADG) was higher and the ratio of feed intake to body weight gain (F:G ratio) was lower in the treatment groups ($P < 0.01$). The 0.50% Leu group showed a significant increase in loin-eye area ($P = 0.03$) and a significant decrease in average backfat thickness (ABT) compared with the CON group ($P = 0.01$).

3.2. Serum biochemistry

To assess the influence of Leu on lipid metabolism, TG, LDL-C, VLDL-C, CHOL, HDL-C, BUN, ALB, TP and GLU in serum were measured. As shown in Table 4, Leu decreased the concentrations of TG, LDL-C, VLDL-C and CHOL related to lipid metabolism compared with the CON ($P < 0.05$), of which TG, CHOL and LDL-C had highly significant differences ($P < 0.01$). However, Leu had no significant effects on serum TP, HDL-C and GLU concentrations compared with CON ($P > 0.05$), except that BUN values were also decreased ($P = 0.01$).

3.3. Serum cytokine concentration

Next, we investigated the effect of Leu on serum cytokine concentrations. The result showed that the levels of IGF1, MSTN, FGF21, leptin, IL-6, and adiponectin in serum were increased and chemerin levels were decreased in the Leu group in comparison with the CON ($P < 0.05$). However, the level of INS was not influenced by Leu ($P = 0.61$) (Table 5).

3.4. Lipid metabolism enzyme activity

We further explored the effects of Leu on lipid metabolism through measuring the key enzyme activities of the backfat and perirenal fat tissue. As listed in Table 6, 0.25% Leu supplementation significantly increased the enzymatic activities of HSL, ACAT and LPL in backfat tissue ($P < 0.01$). The activity of FAS and ACC was

Table 7
Effects of different levels of leucine on fatty acid profile of backfat.

Item[1]	Leucine levels, %			*P*-value
	0	0.25	0.50	
C10:0	0.09 ± 0.00	0.08 ± 0.00	0.09 ± 0.00	0.35
C12:0	0.08 ± 0.00	0.08 ± 0.00	0.08 ± 0.00	0.93
C14:0	1.28 ± 0.03	1.27 ± 0.03	1.32 ± 0.03	0.61
C15:0	0.06 ± 0.00	0.05 ± 0.00	0.05 ± 0.01	0.73
C16:0	24.83 ± 0.54	24.44 ± 0.27	25.33 ± 0.42	0.34
C16:1	2.19 ± 0.09	2.11 ± 0.12	2.09 ± 0.17	0.85
C18:0	14.58 ± 0.65	14.39 ± 0.53	15.91 ± 0.81	0.26
C18:1n9t	0.17 ± 0.01	0.14 ± 0.01	0.15 ± 0.01	0.06
C18:1n9c	38.21 ± 0.33[a]	35.10 ± 0.63[b]	36.90 ± 0.47[b]	<0.01
C18:2n6c	15.10 ± 0.75[b]	18.41 ± 0.83[a]	14.90 ± 0.95[b]	0.02
C20:0	0.25 ± 0.01	0.26 ± 0.01	0.28 ± 0.02	0.47
C20:1	0.86 ± 0.02	0.82 ± 0.03	0.83 ± 0.06	0.80
C18:3n3	0.86 ± 0.06[a]	1.14 ± 0.08[a]	0.77 ± 0.06[b]	<0.01
C20:2	0.69 ± 0.03	0.77 ± 0.03	0.67 ± 0.05	0.16
C20:3n6	0.12 ± 0.01	0.12 ± 0.01	0.12 ± 0.01	0.10
C20:3n3	0.14 ± 0.01	0.15 ± 0.01	0.13 ± 0.01	0.16
C20:4n6	0.31 ± 0.02	0.33 ± 0.01	0.31 ± 0.02	0.86
SFA	41.10 ± 1.14	42.96 ± 1.10	40.57 ± 0.73	0.25
MUFA	41.49 ± 0.40[a]	39.96 ± 0.50[a]	38.17 ± 0.70[b]	<0.01
PUFA	17.15 ± 0.89[b]	16.80 ± 1.10[b]	20.92 ± 0.95[a]	0.02
PUFA:SFA ratio	0.42 ± 0.03[ab]	0.40 ± 0.04[b]	0.52 ± 0.03[a]	0.06

[a, b] Within a row, means without a common superscript are significantly different ($P < 0.05$).
[1] SFA = saturated fatty acid; MUFA = monounsaturated fatty acid; PUFA = polyunsaturated fatty acid.

reduced by 0.50% Leu ($P < 0.05$), whereas the activity of ATGL was not influenced by Leu ($P = 0.76$). Similarly, in perirenal fat, the activities of ACAT and LPL were notably increased by 0.25% Leu ($P < 0.05$), and the activities of FAS, ACC, HSL and ATGL were not influenced ($P > 0.05$).

3.5. Medium-long-chain fatty acids of backfat tissue

As listed in Table 7, palmitic acid (c16:0), oleic acid (c18:1n9c) and linoleic acid (c18:2n6c) were the abundant fatty acids in the backfat tissue. On the whole, only a small portion of fatty acids were influenced by the Leu treatments in backfat tissue. The 0.50% Leu significantly reduced the content of c18:1n9c, c18:3n3 and monounsaturated fatty acids (MUFA) ($P < 0.01$), while 0.25% Leu had no prominent effect on the values of polyunsaturated fatty acid (PUFA) and PUFA to saturated fatty acid (SFA) ratio ($P > 0.05$). The content of PUFA was significantly increased by 0.50% Leu ($P = 0.02$), and the ratio of PUFA to SFA trended upwards ($P = 0.06$).

3.6. Mean diameter and quantity of adipocytes in backfat tissue

To further explored the effect of Leu on lipid metabolism, we performed histological analysis of backfat tissue. As shown in Fig. 1, adipocytes in the three groups were uniform in size and the borders were clear and closely arranged. In the same field of view, compared with the CON, the number of adipocytes in the Leu treatments groups was increased and the diameter of which was smaller ($P < 0.05$).

3.7. Relative mRNA expression levels of the key genes related to lipid metabolism

Next, we validated the effects of Leu-mediated lipid metabolism and measured the relative mRNA expression levels of the key genes in the backfat and perirenal fat tissue. In the backfat tissue, the relative mRNA expression levels of adipocyte synthesis-related genes such as *ACC*, sterol regulatory element binding protein-1c (*SREBP1c*) and *FAS* were significantly reduced by Leu supplementation ($P < 0.05$). The 0.50% Leu group showed a greater impact on the value of *ACC* and *FAS*, while the 0.25% Leu group had greater impact on *SREBP1c* ($P < 0.05$). Furthermore, the 0.50% Leu group had higher expression levels of lipolysis-related genes like *LPL* and *ATGL* than those in the other two groups ($P < 0.05$). However, either 0.25% or 0.50% Leu had no obvious effect on value of *HSL* ($P > 0.05$). In terms of fatty acid transport, 0.25% Leu increased the expression of recombinant fatty acid binding protein 4 (*FABP4*) and fatty acid translocase (*FAT/CD36*) ($P < 0.05$), and decreased the value of recombinant fatty acid transport protein 1 (*FATP1*) ($P < 0.05$). Leu prominently reduced the expression levels of peroxisome proliferator-activated receptor γ (*PPARγ*). Additionally, Leu increased leptin levels and decreased chemerin levels ($P < 0.05$), while the expression levels of adiponectin and resistin were not affected ($P > 0.05$). We further detected the relative mRNA expression levels of SIRT family in the backfat tissue. The expression levels of *SIRT1, SIRT2* and *SIRT5* were prominently increased by 0.25% Leu, while the value of *SIRT4* was reduced ($P < 0.05$). However, *SIRT3* and *SIRT6* were not obviously influenced by dietary Leu treatments ($P > 0.05$).

Similarly, in the perirenal fat tissue, the relative mRNA expression levels of *FAS* and *SREBP1c* were downregulated and the value of LPL was upregulated by 0.25% Leu ($P < 0.05$). Furthermore, 0.25% Leu increased the values of *FABP4* and *FAT/CD36*, but decreased the value of *FATP1*; whereas 0.25% Leu had the most significant effect on *FABP4* ($P < 0.05$). Moreover, 0.25% Leu notably reduced the levels of *PPARγ* and CCAAT enhancer-binding proteinsα (*C/EBPα*) ($P < 0.05$) and observably upregulated the values of adiponectin and downregulated the value of resistin ($P < 0.05$), while there was no effect on leptin and chemerin (Figs. 2–5).

3.8. Relative expression levels of energy metabolism-related key proteins

To verify the energy metabolism signaling pathway involved in Leu treatments, we performed western blotting analysis of key

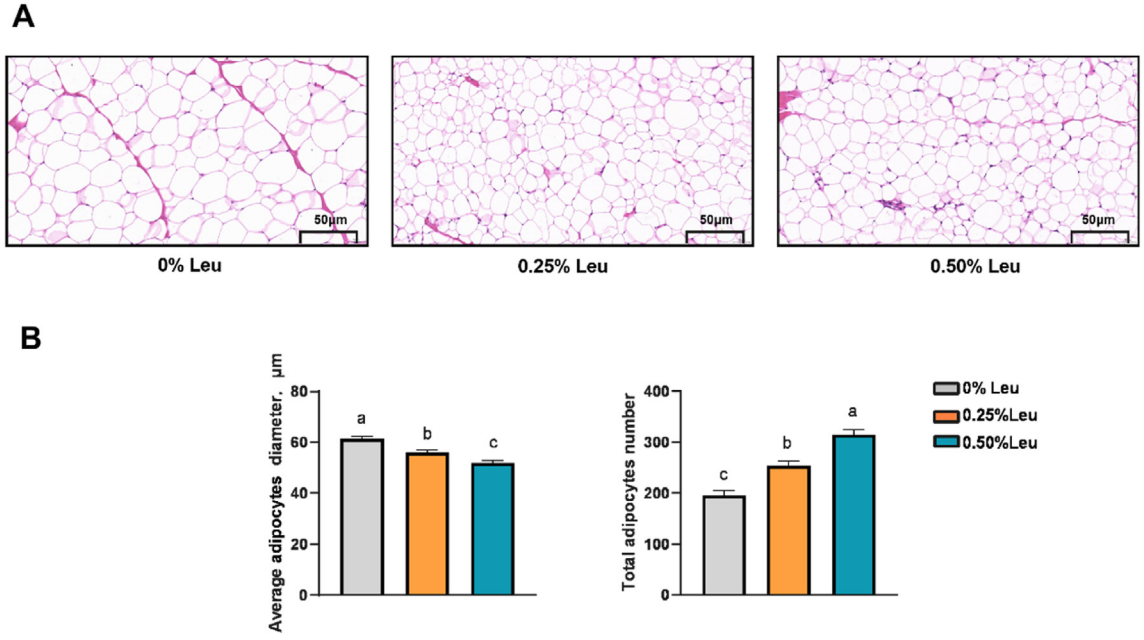

Fig. 1. Histological analysis of the mean diameter area and quantity of adipocytes of finishing pigs fed diets with different levels of leucine. (A) Representative cross-sectional hematoxylin and eosin (H&E) staining photos of adipocytes in backfat tissue (magnification 100× , scale bar = 50 μm); (B) Quantitative analysis mean diameter and adipocyte number in backfat tissue. Data are expressed as means ± SEM. $^{a-c}$ Values with different letters are significantly different among dietary leucine treatments ($P < 0.05$). Leu = leucine.

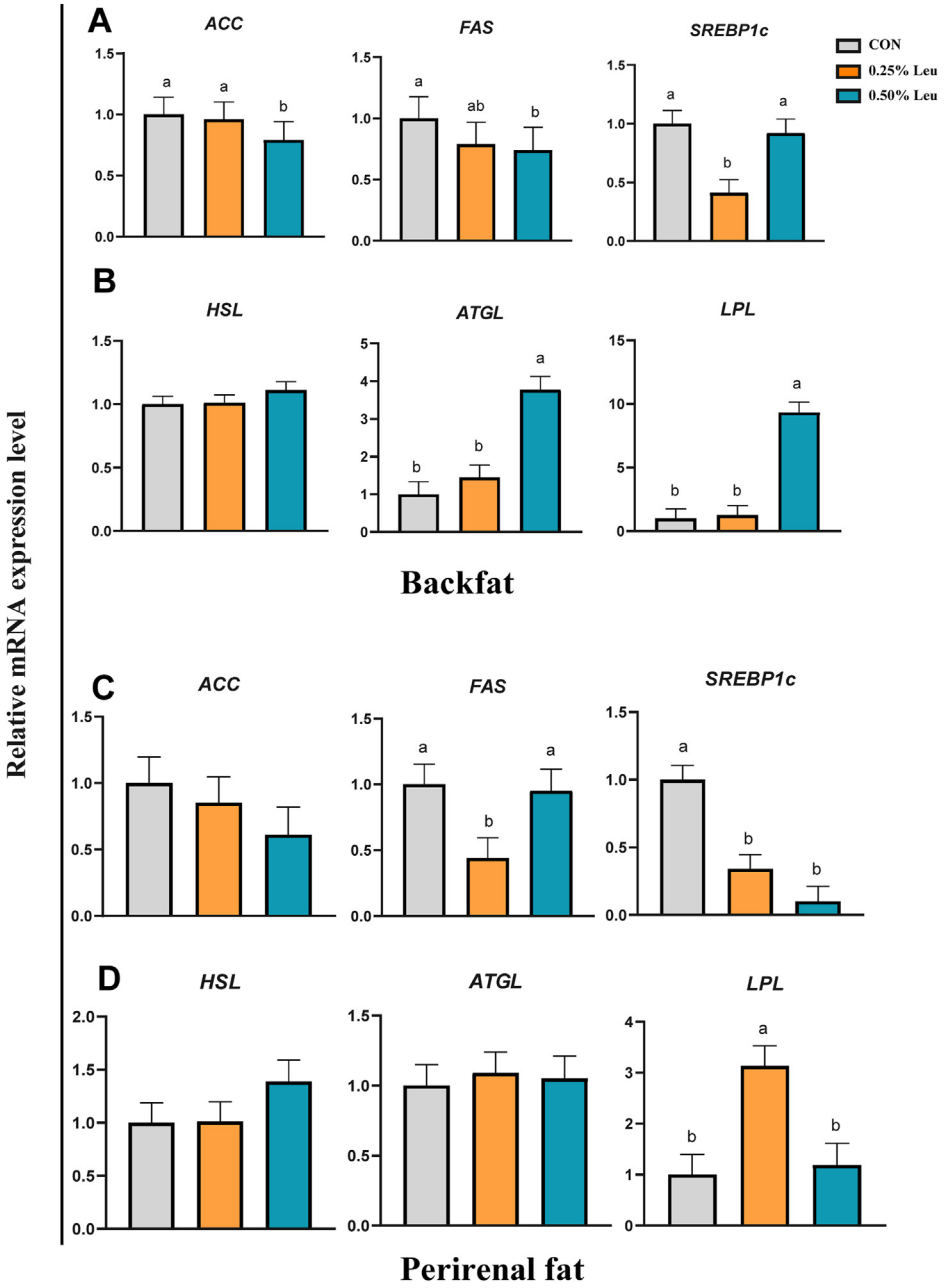

Fig. 2. The relative mRNA expression levels of the key genes related to lipogenesis and lipolysis in adipose tissue. (A) The key genes related to lipogenesis in backfat including acetyl-CoA carboxylase (*ACC*), fatty acid synthase (*FAS*), and sterol regulatory element binding protein-1c (*SREBP1c*); $n = 8$. (B) The key genes related to lipolysis in backfat including hormone-sensitive lipase (*HSL*), lipoprotein lipase (*LPL*) and adipose triacylglyceride lipase (*ATGL*); $n = 8$. (C) The key genes related to lipogenesis in perirenal fat including *ACC*, *FAS* and *SREBP1c*; $n = 8$. (D) The key genes related to lipolysis in perirenal fat including *HSL*, *LPL* and *ATGL*; $n = 8$. Data are expressed as means ± SEM ($n = 8$). Leu = leucine. $^{a, b}$ Bars without a common superscript are significant different ($P < 0.05$).

proteins in backfat tissue. As shown in Fig. 6, 0.25% Leu reduced the expression levels of Ac-silencing information regulator 2 related enzyme 1 (Ac-SIRT1) and p-mammalian target of rapamycin (p-mTOR) compared with the CON, as well increased the value of p-Rictor, p-Raptor, p-inhibitory eIF4E-binding protein 1 (p-4EBP1), p-SIRT1, and Ac-ribosome s6 protein kinase 1 (Ac–S6K1) ($P < 0.05$). In addition, the 0.50% Leu group significantly increased the protein expression level of p-S6K1 compared with the 0.25% Leu group ($P < 0.05$).

3.9. Bacterial development in the colon cavity

Combining the above data, we found that 0.25% Leu had the strongest effect, thus the colon microbiota was measured in this group. The results showed that 0.25% Leu significantly increased the diversity of intestinal microbiota, including Chao1, Observed_species, Shannon, Faith_Phylogenetic Diversity (PD), Good's_Coverage and Pielou_E ($P < 0.05$), but had no effect on Simpson index ($P > 0.05$) (Fig. 7A). Next, we performed principal component

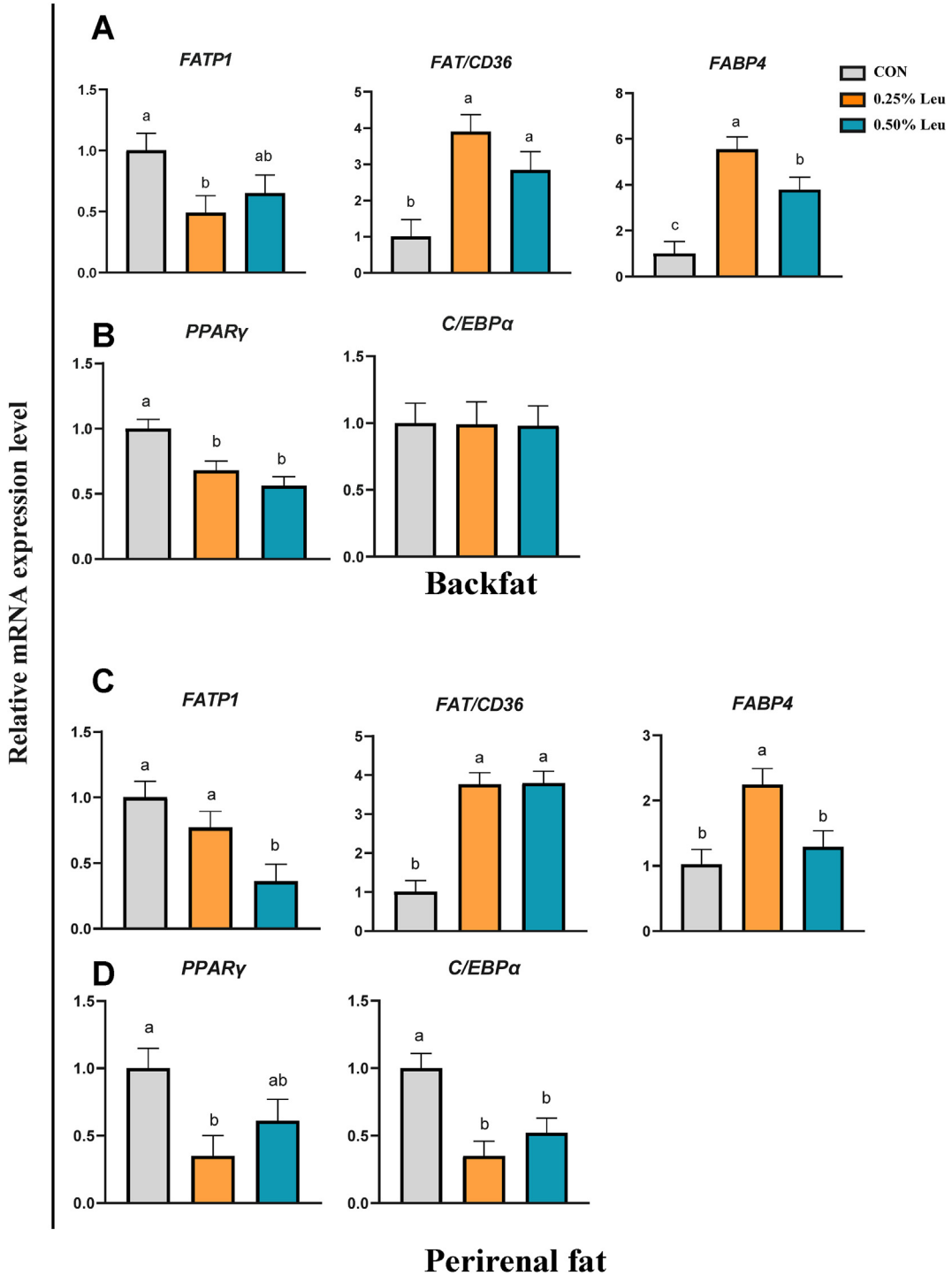

Fig. 3. The relative mRNA expression levels of the key genes related to fatty acid transport and oxidation in adipose tissue. (A) The key genes related to fatty acid transport in backfat including fatty acid transporter protein 1 (*FATP1*), fatty acid translocase (*FAT/CD36*), and fatty acid binding protein 4 (*FABP4*); $n = 8$. (B) The key genes related to fatty acid oxidation in backfat including peroxisome proliferator-activated receptor γ (*PPARγ*) and CCAAT enhancer-binding proteinsα (*C/EBPα*); $n = 8$. (C) The key genes related to fatty acid transport in perirenal fat including *FATP1*, *FAT/CD36* and *FABP4*; $n = 8$. (D) The key genes related to fatty acid oxidation in perirenal fat including *PPARγ* and *C/EBPα*; $n = 8$. Data are expressed as means ± SEM ($n = 8$). $^{a-c}$ Bars without a common superscript are significant different ($P < 0.05$). Leu = leucine.

analysis, which showed that the two groups had different bacterial compositions (Fig. 7B). We analyzed the changes of bacteria at the genus and phylum level. At the phylum level, Firmicutes and Bacteroidetes are the dominant phyla of the two groups, accounting for more than 85% of the total 16S rRNA gene sequence. Among them, the relative abundance of Bacteroidetes in the 0.25% Leu group was notably higher than that in the CON ($P < 0.05$), while that of Firmicutes was dramatically lower than the CON. At the genus level, the relative abundances of *Desulfovibrio* and *Treponema* in the 0.25% Leu group were prominently lower than those in the CON ($P < 0.05$), and *Lactobacillus* and *Shigella* were significantly higher than the CON ($P < 0.05$) (Fig. 7C).

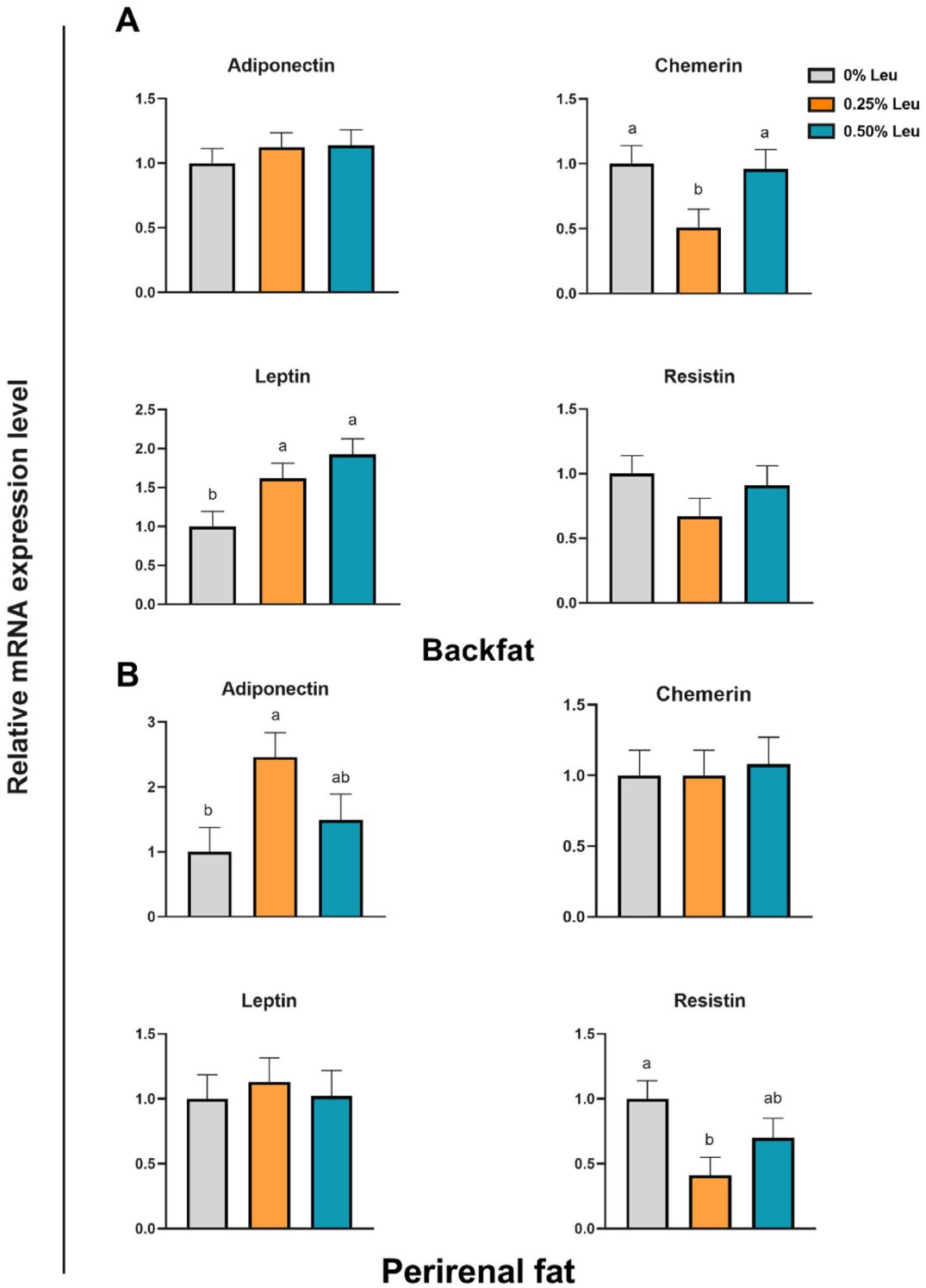

Fig. 4. Relative mRNA expression levels of adipocytokine in backfat (A) and perirenal fat (B). [a, b] Bars without a common superscript are significant different ($P < 0.05$). Leu = leucine.

3.10. Relationship between intestinal microbiota and bile acids

We detected the metabolic spectrum of serum BA. The Orthogonal Partial Least Squares-Discriminant Analysis (OPLS-DA) score showed that there was a clear separation of metabolites of BA between the two groups (Fig. 8A). We screened four metabolites of allolithocholic acid (alloLCA), isolithocholic acid (isoLCA), ursodeoxycholic acid (UDCA) and hyodeoxycholic acid (HDCA) by the standard of variable importance in the project (VIP) > 1, $P < 0.05$ (Fig. 8B). Intestinal microbiota is closely related to bile acid metabolism. Therefore, we conducted further correlation analysis between bile acid differential metabolites, intestinal microbiota and adipokines. The correlation heat map showed that HDCA was negatively correlated with ABT, CHOL and LDL-C, and positively

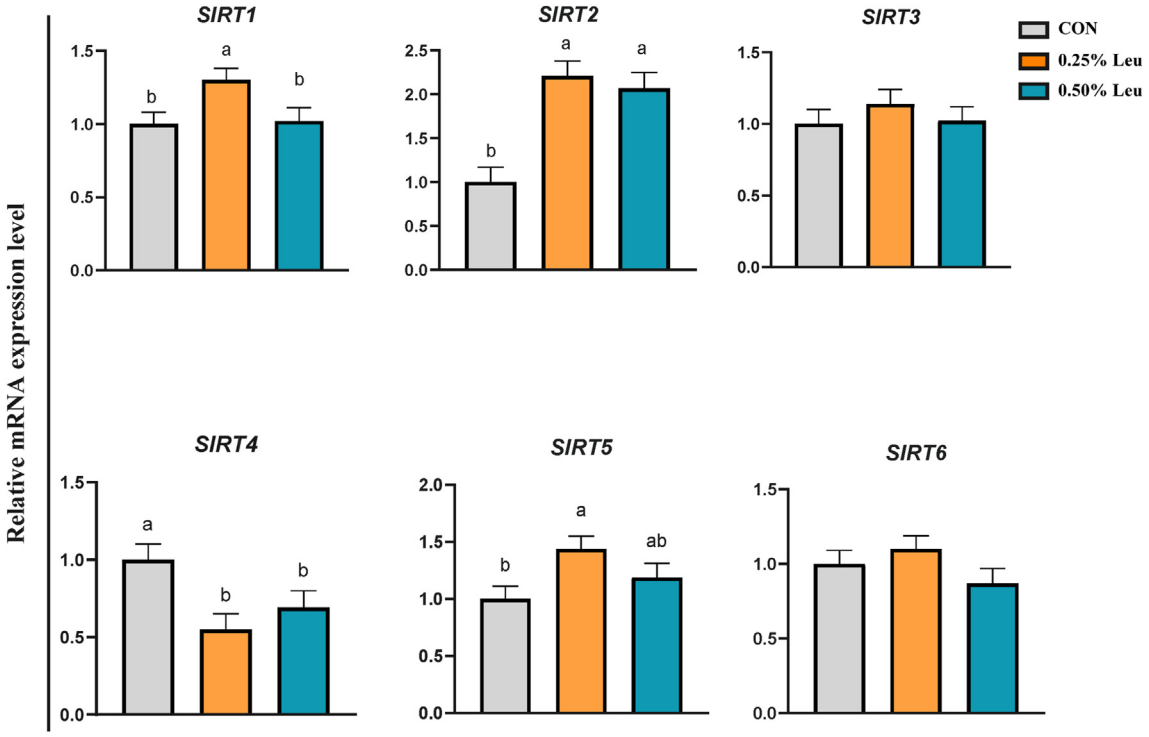

Fig. 5. Relative mRNA expression levels of silent mating type information regulator 2 homolog family (*SIRTs*) in backfat. [a, b] Bars without a common superscript are significant different ($P < 0.05$). Leu = leucine.

correlated with FGF21, IL-6 and *Lactobacillus*. UDCA was negatively correlated with ABT and chemerin, and positively correlated with FGF21, IL-6 and *Lactobacillus*; alloLCA was negatively correlated with *Desulfovibrio*, TG, CHOL, LDL-C and VLDL-C, and positively correlated with IL-6; isoLCA was negatively correlated with *Desulfovibrio*, CHOL, LDL-C and VLDL-C, and significantly positively correlated with *Lactobacillus* (Fig. 8C).

4. Discussion

Studies have shown that dietary Leu can prevent obesity caused by HFD and reduce lipid accumulation in mice (Li et al., 2012). Compared with the CON, dietary Leu significantly increased ADG and decreased F:G ratio of finishing pigs, indicating that Leu could improve the growth performance of finishing pigs. Studies have shown that Leu supplementation can significantly increase duodenal villus height and villus height to crypt depth ratio of weaned piglets. The significant increase in ADG of finishing pigs may be due to the improvement of intestinal structure of finishing pigs by Leu, which promotes the digestion and absorption of nutrients. However, the beneficial effect of Leu on the intestinal tract of fattening pigs needs further study (Sun et al., 2015). High dose dietary supplementation of Leu can reduce feed intake and production performance of pigs, suggesting that dietary supplementation of less than 2% Leu is appropriate (Hyun et al., 2003). Kwon et al. (2019a) showed that the ADFI and ADG of growing pigs were increased by 1% Leu. Excess Leu reduces serotonin concentrations in the plasma and hypothalamus, which may lead to reduced Trp uptake in the brain, which may subsequently affect appetite regulation and negatively affect feed intake (Kwon et al., 2019b). In the present study, Leu supplementation did not significantly affect ADFI of growing pigs, probably because the coordination between small amounts of Leu, valine, isoleucine and tryptophan in the diet had no significant effect on the serotonin production by the hypothalamus. Most studies have focused on the effects of excessive Leu supplementation on hypothalamic serotonin release in piglets or growing pigs, but there are few studies on whether low levels of Leu supplementation promote serotonin release (Kwon et al., 2019b, 2022; Wessels et al., 2016). Average backfat thickness, loin-eye area, lean meat percentage and total fat percentage are important indicators of carcass weight. In this study, 0.50% Leu supplementation significantly increased loin-eye area and decreased backfat thickness in finishing pigs (Giovannini and Bianchi, 2017). These results suggest that Leu has a potential inhibitory effect on the deposition of backfat.

Dietary Leu reduces hyperglycemia and high cholesterol caused by HFD and reduces the rate of fat production in the body (Liu et al., 2017; Manders et al., 2006). Duan et al. (2018) found that the addition of appropriate proportion of BCAAs in a low protein diet (1:0.75:0.75 to 1:0.25:0.25) improved growth performance of growing pigs, and regulated fatty acid synthesis, transport and oxidation, lipolysis and adipokine secretion through AMPK-mTOR pathway (Duan et al., 2018). CHOL and TG concentrations in serum reflect the dynamic fat absorption and nutritional status in animals. Studies have shown that CHOL and LDL-C levels are positively correlated with body fat deposition and the incidence of coronary heart disease. VLDL-C is described as an atherogenic factor, LDL-C is the main carrier of CHOL and an important marker of excessive CHOL deposition in the body (Brown et al., 2006). Also, we demonstrated that Leu plays a key role in improving both lipid metabolism and cardiovascular health in the finishing pigs, as supported by reducing serum concentrations of TG, LDL-C, VLDL-C and CHOL, similar results were also found in mice (Jiao et al., 2016; Ma et al., 2020).

Adipokines are secreted by white fat and play a key role in energy distribution (Muoio and Newgard, 2005). Studies have shown that FGF21 (Coskun et al., 2008), IGF1 (Mauras et al., 2000) and adiponectin (Yanai and Yoshida, 2019) can enhance adipose tissue

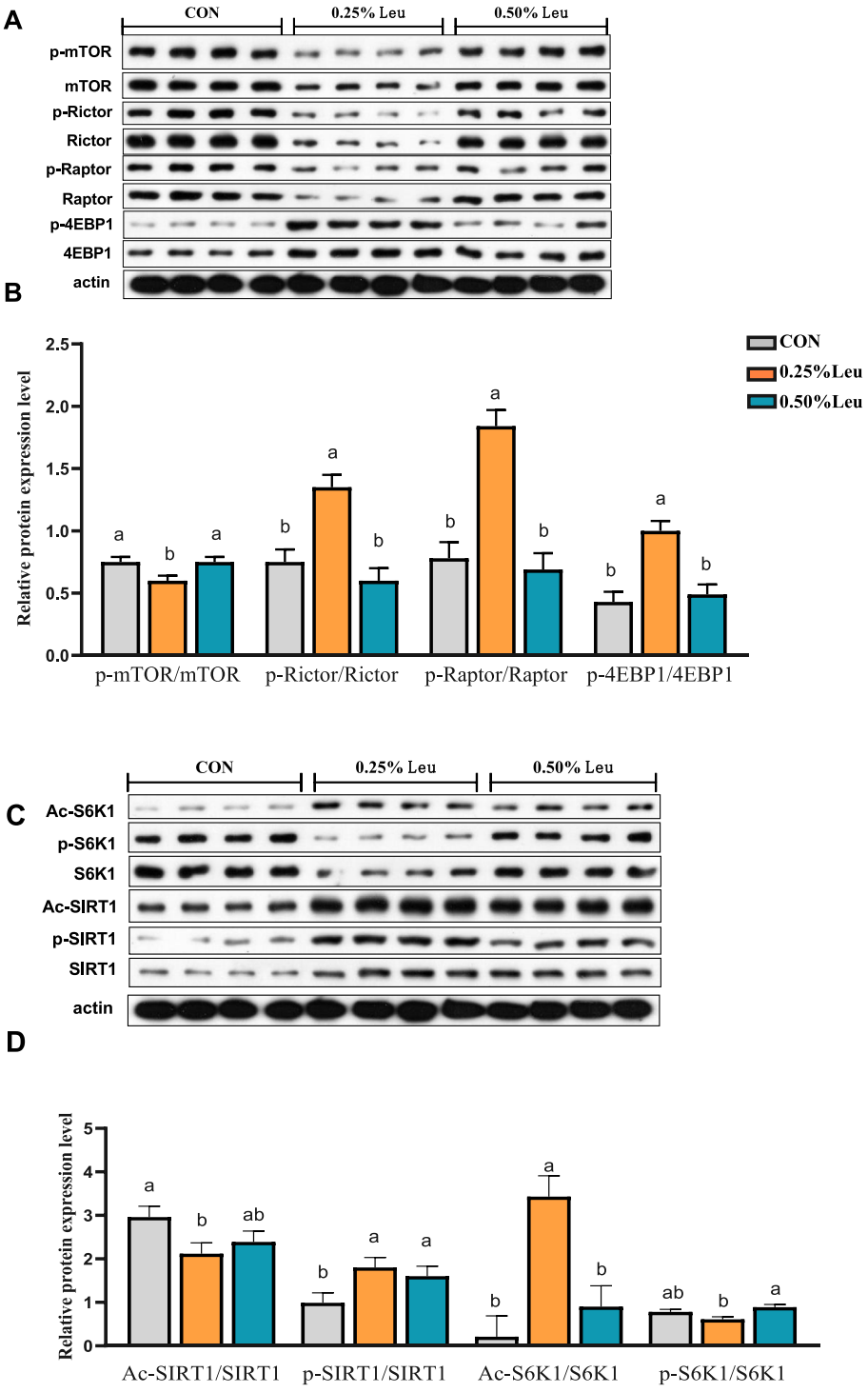

Fig. 6. Representative immunoblots of protein levels, acetylation and phosphorylation degrees in backfat tissue of finishing pigs. Data are expressed as means ± SEM. [a,b] Bars without a common superscript are significant different ($P < 0.05$). Leu = leucine; mTOR = mammalian target of rapamycin; 4EBP1 = inhibitory eIF4E-binding protein 1; SIRT1 = silent mating type information regulator 2 homolog 1; S6K1 = ribosome s6 protein kinase 1.

lipolysis and increase the rate of lipid oxidation; MSTN (Pan et al., 2021), leptin (Funcke and Scherer, 2019) and IL-6 (Wallenius et al., 2002) reduce lipid accumulation in tissues; chemerin (Goralski et al., 2007) and resistin (Ikeda et al., 2013) can regulate adipogenesis and adipocyte metabolism. Yuan et al. (2015) showed that Leu can significantly increase the secretion of leptin in adipocytes through the mTOR signaling pathway and reduce the occurrence of obesity. In the present study, 0.25% Leu markedly decreased the concentration of chemerin in serum; in agreement with these results, chemerin mRNA expression levels in backfat showed a similar trend. At the same time, the serum concentrations of FGF21, IGF1, MSTN, IL-6, leptin and adiponectin increased. In

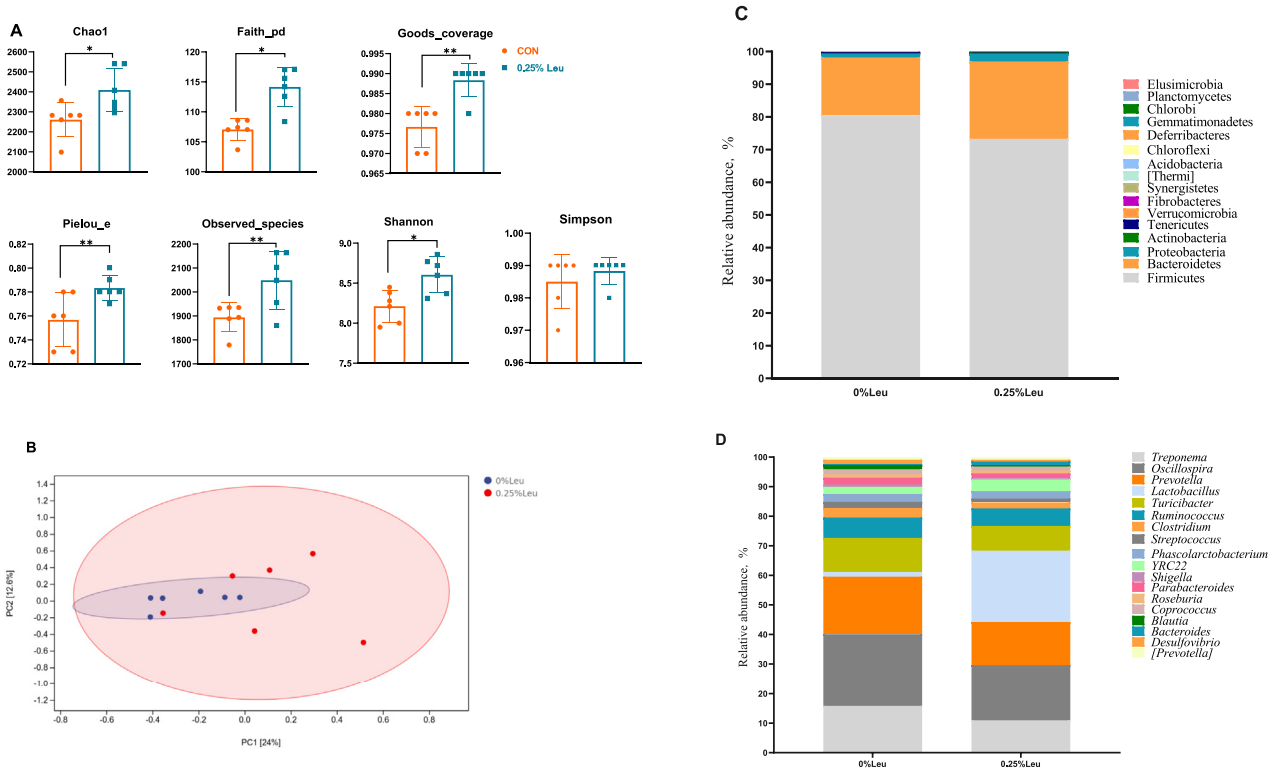

Fig. 7. Microbial development in the chyme. (A) α-Diversity and (B) β-diversity, (C and D) bacterial species enriched in finishing pigs. The data were assessed using *t*-test by comparing the 0% and 0.25% leucine in finishing pigs using SPSS 20.0. Figures were drawn using GraphPad Prism 8.0. Values are presented as the means ± SEM. *, $P < 0.05$, **, $P < 0.01$. Leu = leucine.

addition, adiponectin and MSTN also play a role in reducing TG levels, which further explains the decrease of serum TG level. Notably, the results also suggested a positive effect of Leu on lipid metabolism through significant changes in adipokine gene expression in backfat and perirenal fat, such as increasing the levels of leptin in backfat, reducing the value of resistin in perirenal fat, and so on. These results suggest that Leu (especially 0.25%) regulate lipid metabolism by improving adipokine secretion and expression levels in finishing pigs.

We investigated the effect of Leu on fatty acid composition, and found that 0.50% Leu supplementation reduced the content of MUFA and PUFA. *SREBP1c* is not only involved in lipid biosynthesis and accumulation, but also in fatty acid oxidation (Hagen et al., 2010). Therefore, Leu may down-regulate MUFA and PUFA content through *SREBP1c*, which was confirmed by the reduction of *SREBP1c* relative mRNA expression levels in the backfat tissue. After the formation of medium-long-chain fatty acids, they are incorporated into TG and phospholipids in many possible combinations, so that the TG content in serum also decreased (Hagen et al., 2010). In our study, the relative mRNA expression levels of *FATP1* in backfat and perirenal fat decreased, while the value of *FABP4* and *FAT/CD36* increased. The low expression level of *FATP1* promotes fatty acid oxidation, which also reduces lipid accumulation in tissues (Huang et al., 2021). Previous studies have shown that overexpression of *FATP1* in pigs' intramuscular preadipocytes observably increased the expression levels of *PPARγ*, *C/EBPα* and *FAS* (Chen et al., 2017). The present study also indicated that Leu decreased the expression levels of *PPARγ*, *C/EBPα* and *FAS* and might suppress the expression of *FATP1*.

Fat deposition is mediated by a complex balance of lipogenic and lipolytic enzymes. HSL and ATGL are two essential lipases, and ACC is a rate-limiting enzyme in animals (Tong, 2005). HSL hydrolyzes lipids such as TG, diglycerides and monoglycerides to produce glycerol and free fatty acids (FFA) (Yeaman, 1990, 2004). ATGL is highly expressed in adipose tissue and is specific to TG (Zimmermann et al., 2004). LPL can degrade TG in the serum to glycerol and FFA (Havel, 2010), and FAS catalyzes de novo synthesis of fatty acids (Jensen-Urstad and Semenkovich, 2012). Furthermore, ACAT is the only enzyme that catalyzes the production of cholesteryl esters from cholesterol, and excess cholesteryl esters may contribute to atherosclerosis (Lopez-Farre et al., 2008). Therefore, Leu suppresses fat deposition and reduces the serum TG levels as evidenced by the enhanced activities of HSL and LPL, as well as decreased enzyme activity and relative mRNA expression levels of *FAS* in the backfat tissue in agreement with perirenal fat tissues. Studies have found that *SREBP1* regulates the expression of FAS, LPL, and ACC involved in lipid biosynthesis (Hagen et al., 2010). Hence, these results suggest that Leu might regulate the expression levels of *FAS, LPL* and *ACC* by suppressing the expression of *SREBP1c*.

Sirtuins are NAD^+-dependent histone deacetylases that regulate vital metabolic pathways in prokaryotes and eukaryotes and participate in many biological processes including cell metabolism and caloric restriction. We found that 0.25% Leu promoted lipolysis and inhibited fat synthesis and fat storage as demonstrated by the increase in mRNA expression levels of *SIRT1*, which inhibited the expression levels of *PPARγ* and *SREBP1* in backfat tissue (Carafa et al., 2016). We showed that 0.25% Leu markedly downregulated the expression of *SIRT4*, which may regulate lipid metabolism and fatty acid oxidation in vivo by activating *PPARα* activity through *SIRT1* (Laurent et al., 2013; Nasrin et al., 2010). Furthermore, we found that 0.25% Leu could reduce fat accumulation in backfat, which was supported by overexpression of *SIRT5*, which can

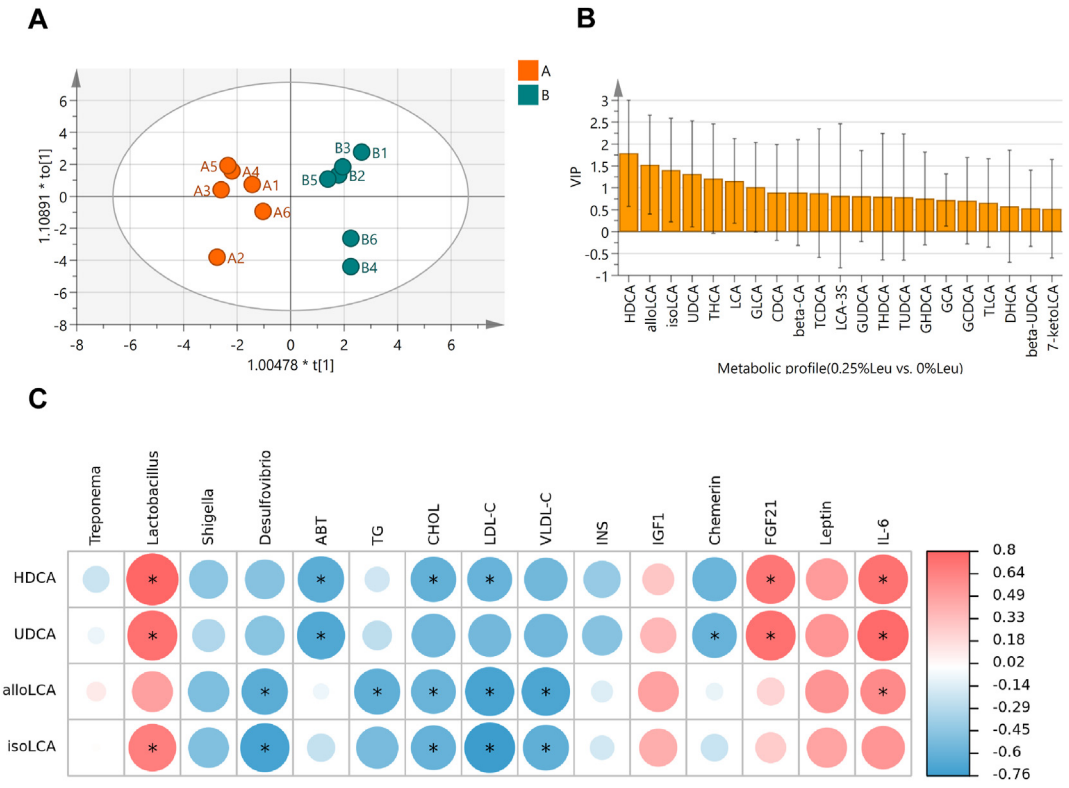

Fig. 8. Serum bile acid metabolic profile and correlation analysis. (A) Orthogonal Partial Least Squares-Discriminant Analysis (OPLS-DA) score. Leu = leucine. Orange legend A represents 0% leucine and green legend B represents 0.25% leucine. (B) Bile acid (BA) metabolic profile. VIP = variable importance in the projection; HDCA = hyodeoxycholic acid; alloLCA = allolithocholic acid; isoLCA = isolithocholic acid; UDCA = ursodeoxycholic acid; THCA = taurocholic acid sodium salt; LCA = lithocholic acid; GLCA = glycinocholate sodium salt; CDCA = chenodeoxycholic acid; beta-CA = 3 beta-cholic acid; TCDCA = taurocholic acid; LCA-3S = taurocholate 3-sulfate disodium salt; GUDCA = glycyrsodesoxycholic acid; THDCA = taurodeoxycholic acid; TUDCA = tauroursodeoxycholic acid; GHDCA = glycine hyodeoxycholic acid; GCA = glycocholic acid; GCDCA = deoxycholic acid sodium salt; TLCA = taurocholate sodium salt; DHCA = dehydrocholic acid; beta-UDCA = 3 beta-ursodeoxycholic acid; 7-ketoLCA = 7-ketocholic acid. (C) Correlation analysis of bile acid metabolites and lipid metabolism. We screened 4 metabolites with VIP > 1 and $P < 0.05$ as standards, and then Spearman correlation analysis was performed with 11 different bacteria. *, $P < 0.05$. ABT = average backfat thickness; TG = triglyceride; CHOL = cholesterol; VLDL-C = very low-density lipoprotein cholesterol; LDL-C = low-density lipoprotein cholesterol; INS = insulin; IGF1 = insulin-like growth factor 1; FGF21 = fibroblast growth factor 21; IL-6 = interleukin 6.

notably suppress the expression levels of *PPARγ*, *FAS*, *ACC* in the AMPK signaling pathway and inhibit preadipocyte differentiation and lipid synthesis (Hong et al., 2020).

mTOR plays a critical role in cell growth, apoptosis, autophagy and metabolism (Shan et al., 2016), including two separate complexes mTORC1/2. mTORC1 consists of mTOR, raptor and mLST8/GβL, and its main downstream effectors are ribosomal S6 kinase (S6K1) and inhibitory eIF4E-binding protein (4EBPs) (Mao and Zhang, 2018). mTORC2 and its core component rictor are key controllers of lipid metabolism (Cybulski et al., 2009). The results of this study showed that 0.25% Leu inhibited the phosphorylation protein levels of mTOR, which promoted the terminal differentiation of preadipocytes to mature adipocytes by activating the phosphorylation of its direct substrate 4EBPs and PPARγ (Le Bacquer et al., 2007; Lefterova et al., 2014), while inhibiting the phosphorylation of S6K1,thus increasing the rate of lipolysis (Carnevalli et al., 2010). Similarly, 0.25% Leu increased the phosphorylation of raptor, which is involved in the formation of lipid-rich adipocytes (Martin et al., 2015). Moreover, 0.25% Leu controls adipogenesis by activating the phosphorylation levels of rictor. SIRT1-inhibition induces acetylation of S6K1 and suppresses mTOR-dependent phosphorylation of S6K1 (Hong et al., 2014). Our results show that Leu promotes fatty acid oxidation as evidenced by increased levels of SIRT1 protein phosphorylation and modulations in the mTOR signaling pathway. This further confirms the interaction between mTOR and SIRT1 in the process of lipid metabolism, which is in agreement with the research of Giovannini and Bianchi (2017). Therefore, Leu may regulate lipid metabolism through the mTOR-SIRT1 signaling pathway in finishing pigs. Interestingly, leptin expression is also increased in cells that are continuously activated by mTORC1 (Zhang et al., 2009), which regulates FGF21 expression in liver, while its role in regulating FGF21 production in adipose tissue remains to be determined (Cornu et al., 2014). Lipid-specific knockdown of rictor was demonstrated to reduce serum adiponectin levels in mice and regulate liver IGF1 secretion and ultimately lead to systemic metabolic alterations (Cybulski et al., 2009). Considering that Leu dramatically changed FGF21, leptin, and adiponectin, we hypothesized that Leu might be involved in adipokine biosynthesis and/or secretion in vivo through the mTOR signaling pathway.

Importantly, intestinal microbiota influence lipid levels and lipid metabolism in the serum (Zhao et al., 2021). Firmicutes, known as the bacterial phylum associated with obesity, accelerates the degradation of food components to provide energy for the host (Khan et al., 2016). A high abundance of Firmicutes and a low abundance of Bacteroides result in accelerated energy acquisition from food promoting energy accumulation in host adipose tissue, which further inhibits fasting-induced adipose factor (FIAF) production (Angelakis et al., 2012). As a result, higher TG is stored in adipose tissue and lower levels of satiety hormones are released (Crovesy et al., 2017). Firmicutes inhibits the release of LPL inhibitors, increases LPL activity, and promotes the storage of excess energy into fat (Dridi et al., 2011). Therefore, we hypothesized that TG and LPL may be impacted by Leu through reducing the relative

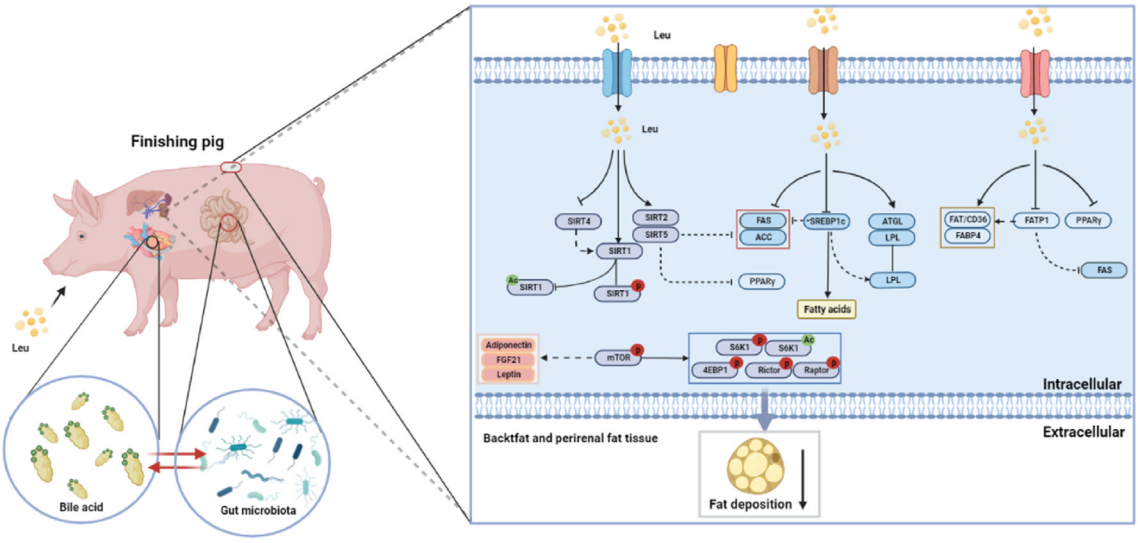

Fig. 9. Leu regulates lipid metabolism in white adipose tissue through adipokine-mTOR-SIRT1 signaling pathway and bile acid–microbiota axis in a finishing pig model. Leu = Leucine; SIRT = silent mating type information regulator 2 homolog family; FAS = fatty acid synthase; ACC = acetyl CoA carboxylase; SREBP-1c = sterol regulatory element binding protein-1c; ATGL = adipose triacylglyceride lipase; LPL = lipoprotein lipase; FAT/CD36 = fatty acid translocase; FABP4 = fatty acid binding protein 4; FATP1 = fatty acid transport protein 1; PPARγ = peroxisome proliferator-activated receptor γ; FGF21 = fibroblast growth factor 21; mTOR = mammalian target of rapamycin; 4EBP1 = inhibitory eIF4E-binding protein1 S6K1 = ribosome s6 protein kinase.

abundance of Firmicutes and enhancing the abundance of Bacteroides, promoting FIAF production and the release of more satiety hormones so as to reduce food consumption. *Desulfovibrio* is a sulfate-reducing bacterium that produces LPS and induces associated inflammation (Li et al., 2021; Wang et al., 2020). *Treponema* correlates with digestibility of crude fiber in pigs (Niu et al., 2015). Although members of the genus may be pathogenic, they may also be symbiotic (Rosewarne et al., 2012). Leu might improve intestinal inflammation by reducing *Desulfovibrio* and *Treponema*. Based on our results, we believe that the increase of ADG and feed efficiency is due to the influence of Leu on the abundance of *Lactobacillus* and *Shigella*. This is mainly due to the fact that *Lactobacillus*, considered a probiotic (Valeriano et al., 2017) whose abundance is higher in the cecum and feces of pigs with more efficient diets (Vigors et al., 2016; Yang et al., 2017a), and *Shigella* was inversely associated with ADG and carcass weight (Torres-Pitarch et al., 2020). Bile acid (BA) is an effective "digestive surfactant" through activating various signaling pathways. BA not only regulates its own synthesis and enterohepatic circulation, but also contributes to the maintenance of TG, cholesterol, glucose and energy homeostasis (Staels and Fonseca, 2009). In addition, intestinal microbiota can bind BA to cholesterol molecules and excrete BA-cholesterol complexes in feces (Khan et al., 2018). HDCA reduces serum levels of VLDL-C and LDL-C cholesterol (Sehayek et al., 2001). We suggest that Leu may reduce serum CHOL and LDL-C and reduce fat deposition through HDCA. In addition, UDCA increased *SIRT1* levels and decreased *SREBP-1* levels in mouse adipose tissue (Chen et al., 2019; Hu et al., 2019). UDCA was found to alter BA and cholesterol synthesis by inducing several BA and cholesterol synthesis markers and enzymes such as FXR and CYP7A1 and liver SREBP1 and TGR5 in obese mice (Chen et al., 2019). In this study, 0.25% Leu has a significant effect on SIRT1 and SREBP-1, suggesting that UDCA-SIRT1-SREBP-1 is one of the pathways through which Leu regulates lipid metabolism. In the present study, *Lactobacillus* was positively associated with UDCA and HDCA, in agreement with previous research. UDCA acts through G protein-coupled bile acid receptor 1 (GPBAR1) to enhance BAT activation and non-shivering thermogenesis (Bianco et al., 1988), and it has also been identified as a GPBAR1 agonist (Carino et al., 2019). Activation of GPBAR1 reduces a variety of metabolic and immune abnormalities associated with obesity and diabetes (Wang et al., 2016; Zambad et al., 2013). Moreover, *Desulfovibrio* was negatively correlated with isoLCA and alloLCA, while *Lactobacillus* was positively correlated with isoLCA, alloLCA was negatively correlated with TG, CHOL, LDL-C and VLDL-C, and positively correlated with IL-6. The isoLCA was negatively correlated with CHOL, LDL-C and VLDL-C. The mechanism of isoLCA and alloLCA in regulating body lipid metabolism remains to be elucidated, but the overall data suggested that the intestinal microbiota-bile acid axis is involved in Leu regulating lipid metabolism in finishing pigs.

5. Conclusion

In conclusion, dietary Leu supplementation (especially 0.25%) improved the growth performance and carcass traits of finishing pigs. Leu also reduced body fat deposition in backfat and perirenal fat tissue by regulating the lipid metabolism-related enzyme activity and expression levels of the key genes, with the involvement of adipokine-mTOR-SIRT1 and BA-microbe axis (Fig. 9). Leu supplementation can be an effective nutritional strategy to inhibit adipose deposition in livestock.

Author contributions

Liu Guo: Data curation. **Yehui Duan:** Data curation. **Saiming Gong:** Formal analysis. **Fengna Li:** Funding acquisition. **Qinghua Chen:** Funding acquisition. **Mengmeng Han:** Investigation. **Jingzun Wang:** Methodology. **Hanjing Shi:** Methodology. **Qiuping Guo:** Project administration. **Xianji Jiang:** Project administration. **Yunju Yin:** Writing – original draft.

Declaration of competing interest

We declare that we have no financial and personal relationships with other people or organizations that can inappropriately influence our work, and there is no professional or other personal interest of any nature or kind in any product, service and/or company that could be construed as influencing the content of this paper.

Acknowledgments

We thank all the members of the institute of subtropical agriculture, the Chinese academy of sciences who make efforts to these experiments. This work was supported by National Natural Science Foundation of China (31972582, U22A20516), Science and Technology Innovation Program of Hunan Province (2021RC4039), Key R & D Program of Hunan Province (2022NK2026), the Youth Innovation Promotion Association CAS (Y202079).

References

Angelakis E, Armougom F, Million M, Raoult D. The relationship between gut microbiota and weight gain in humans. Future Microbiol 2012;7:91–109. https://doi.org/10.2217/Fmb.11.142.

Anthony JC, Yoshizawa F, Anthony TG, Vary TC, Jefferson LS, Kimball SR. Leucine stimulates translation initiation in skeletal muscle of postabsorptive rats via a rapamycin-sensitive pathway. J Nutr 2000;130:2413–9.

Atherton PJ, Smith K, Etheridge T, Rankin D, Rennie MJ. Distinct anabolic signalling responses to amino acids in C2C12 skeletal muscle cells. Amino Acids 2010;38:1533–9. https://doi.org/10.1007/s00726-009-0377-x.

Bhargava P, Smith MD, Mische L, Harrington E, Fitzgerald KC, Martin K, Kim S, Reyes AA, Gonzalez-Cardona J, Volsko C, et al. Bile acid metabolism is altered in multiple sclerosis and supplementation ameliorates neuroinflammation. J Clin Invest 2020;130:3467–82. https://doi.org/10.1172/Jci129401.

Bianchi S, Giovannini L. Inhibition of mTOR/S6K1/4E-BP1 signaling by nutraceutical SIRT1 modulators. Nutr Cancer 2018;70:490–501. https://doi.org/10.1080/01635581.2018.1446093.

Bianco AC, Sheng XY, Silva JE. Triiodothyronine amplifies norepinephrine stimulation of uncoupling protein gene transcription by a mechanism not requiring protein synthesis. J Biol Chem 1988;263:18168–75. https://doi.org/10.1016/s0021-9258(19)81340-6.

Brown BG, Stukovsky KH, Zhao XQ. Simultaneous low-density lipoprotein-C lowering and high-density lipoprotein-C elevation for optimum cardiovascular disease prevention with various drug classes, and their combinations: a meta-analysis of 23 randomized lipid trials. Curr Opin Lipidol 2006;17:631–6. https://doi.org/10.1097/MOL.0b013e32800ff750.

Carafa V, Rotili D, Forgione M, Cuomo F, Serretiello E, Hailu GS, Jarho E, Lahtela-Kakkonen M, Mai A, Altucci L. Sirtuin functions and modulation: from chemistry to the clinic. Clin Epigenet 2016;8. https://doi.org/10.1186/s13148-016-0224-3.

Carino A, Biagioli M, Marchiano S, Fiorucci C, Zampella A, Monti MC, Scarpelli P, Ricci P, Distrutti E, Fiorucci S. Ursodeoxycholic acid is a GPBAR1 agonist and resets liver/intestinal FXR signaling in a model of diet-induced dysbiosis and NASH. Biochim Biophys Acta Mol Cell Biol Lipids 2019;1864:1422–37. https://doi.org/10.1016/j.bbalip.2019.07.006.

Carnevalli LS, Masuda K, Frigerio F, Le Bacquer O, Um SH, Gandin V, Topisirovic I, Sonenberg N, Thomas G, Kozma SC. S6K1 plays a critical role in early adipocyte differentiation. Dev Cell 2010;18:763–74. https://doi.org/10.1016/j.devcel.2010.02.018.

Chen XL, Luo YL, Wang RS, Zhou B, Huang ZQ, Jia G, Zhao H, Liu GM. Effects of fatty acid transport protein 1 on proliferation and differentiation of porcine intramuscular preadipocytes. Anim Sci J 2017;88:731–8. https://doi.org/10.1111/asj.12701.

Chen YS, Liu HM, Lee TY. Ursodeoxycholic acid regulates hepatic energy homeostasis and white adipose tissue macrophages polarization in leptin-deficiency obese mice. Cells 2019;8. https://doi.org/10.3390/cells8030253.

China National Standard. Determination of crude protein in feeds-Kjeldahl method No. GB/T 6432-2018. In: Beijing: Standards Press of China; 2018.

Cornu M, Oppliger W, Albert V, Robitaille AM, Trapani F, Quagliata L, Fuhrer T, Sauer U, Terracciano L, Hall MN. Hepatic mTORC1 controls locomotor activity, body temperature, and lipid metabolism through FGF21. P Natl Acad Sci USA 2014;111:11592–9. https://doi.org/10.1073/pnas.1412047111.

Coskun T, Bina HA, Schneider MA, Dunbar JD, Hu CC, Chen YY, Moller DE, Kharitonenkov A. Fibroblast growth factor 21 corrects obesity in mice. Endocrinology 2008;149:6018–27. https://doi.org/10.1210/en.2008-0816.

Crovesy L, Ostrowski M, Ferreira DMTP, Rosado EL, Soares-Mota M. Effect of Lactobacillus on body weight and body fat in overweight subjects: a systematic review of randomized controlled clinical trials. Int J Obes 2017;41:1607–14. https://doi.org/10.1038/ijo.2017.161.

Cybulski N, Polak P, Auwerx J, Ruegg MA, Hall MN. mTOR complex 2 in adipose tissue negatively controls whole-body growth. P Natl Acad Sci USA 2009;106:9902–7. https://doi.org/10.1073/pnas.0811321106.

Dridi B, Raoult D, Drancourt M. Archaea as emerging organisms in complex human microbiomes. Anaerobe 2011;17:56–63. https://doi.org/10.1016/j.anaerobe.2011.03.001.

Duan Yehui, Li, Fengna, Guo, Qiuping, Wang Wenlong, Zhang, Foods LJJoF. Branched-chain amino acid ratios modulate lipid metabolism in adipose tissues of growing pigs. 2018.

Funcke JB, Scherer PE. Beyond adiponectin and leptin: adipose tissue-derived mediators of inter-organ communication. JLR (J Lipid Res) 2019;60:1648–97. https://doi.org/10.1194/jlr.R094060.

Giovannini L, Bianchi S. Role of nutraceutical SIRT1 modulators in AMPK and mTOR pathway: evidence of a synergistic effect. Nutrition 2017;34:82–96. https://doi.org/10.1016/j.nut.2016.09.008.

Goralski KB, McCarthy TC, Hanniman EA, Zabel BA, Butcher EC, Parlee SD, Muruganandan S, Sinal CJ. Chemerin, a novel adipokine that regulates adipogenesis and adipocyte metabolism. J Biol Chem 2007;282:28175–88. https://doi.org/10.1074/jbc.M700793200.

Hagen RM, Rodriguez-Cuenca S, Vidal-Puig A. An allostatic control of membrane lipid composition by SREBP1. FEBS Lett 2010;584:2689–98. https://doi.org/10.1016/j.febslet.2010.04.004.

Havel RJ. Triglyceride-rich lipoproteins and plasma lipid transport. Arterioscl Throm Vas 2010;30:9–19. https://doi.org/10.1161/Atvbaha.108.178756.

He L, Prodhan MAI, Yuan F, Yin X, Lorkiewicz PK, Wei X, Feng W, McClain C, Zhang X. Simultaneous quantification of straight-chain and branched-chain short chain fatty acids by gas chromatography mass spectrometry. J Chromatogr, B: Anal Technol Biomed Life Sci 2018;1092:359–67. https://doi.org/10.1016/j.jchromb.2018.06.028.

Hong JY, Mei CG, Raza SHA, Khan R, Cheng G, Zan LS. SIRT5 inhibits bovine preadipocyte differentiation and lipid deposition by activating AMPK and repressing MAPK signal pathways. Genomics 2020;112:1065–76. https://doi.org/10.1016/j.ygeno.2019.12.004.

Hong SK, Zhao B, Lombard DB, Fingar DC, Inoki K. Cross-talk between sirtuin and mammalian target of rapamycin complex 1 (mTORC1) signaling in the regulation of S6 kinase 1 (S6K1) phosphorylation. J Biol Chem 2014;289:13132–41. https://doi.org/10.1074/jbc.M113.520734.

Hu J, Hong W, Yao KN, Zhu XH, Chen ZY, Ye L. Ursodeoxycholic acid ameliorates hepatic lipid metabolism in LO2 cells by regulating the AKT/mTOR/SREBP-1 signaling pathway. World J Gastroenterol 2019;25:1492–501. https://doi.org/10.3748/wjg.v25.i12.1492.

Hu T, An ZL, Shi C, Li PF, Liu LH. A sensitive and efficient method for simultaneous profiling of bile acids and fatty acids by UPLC-MS/MS. J Pharmaceut Biomed 2020;178. https://doi.org/ARTN 11281510.1016/j.jpba.2019.112815.

Huang JP, Zhu RR, Shi DS. The role of FATP1 in lipid accumulation: a review. Mol Cell Biochem 2021;476:1897–903. https://doi.org/10.1007/s11010-021-04057-w.

Hyun Y, Ellis M, McKeith FK, Baker DH. Effect of dietary leucine level on growth performance, and carcass and meat quality in finishing pigs. Can J Anim Sci 2003;83:315–8. https://doi.org/10.4141/A02-035.

Ikeda Y, Tsuchiya H, Hama S, Kajimoto K, Kogure K. Resistin affects lipid metabolism during adipocyte maturation of 3T3-L1 cells. FEBS J 2013;280:5884–95. https://doi.org/10.1111/febs.12514.

Jensen-Urstad AP, Semenkovich CF. Fatty acid synthase and liver triglyceride metabolism: housekeeper or messenger? Biochim Biophys Acta 2012;1821:747–53. https://doi.org/10.1016/j.bbalip.2011.09.017.

Jiao J, Han SF, Zhang W, Xu JY, Tong X, Yin XB, Yuan LX, Qin LQ. Chronic leucine supplementation improves lipid metabolism in C57BL/6J mice fed with a high-fat/cholesterol diet. Food Nutr Res 2016;60. https://doi.org/10.3402/fnr.v60.31304.

Khan MJ, Gerasimidis K, Edwards CA, Shaikh MG. Role of gut microbiota in the aetiology of obesity: proposed mechanisms and review of the literature. J Obes 2016:7353642. https://doi.org/10.1155/2016/7353642. 2016.

Khan TJ, Ahmed YM, Zamzami MA, Mohamed SA, Khan I, Baothman OAS, Mehanna MG, Yasir M. Effect of atorvastatin on the gut microbiota of high fat diet-induced hypercholesterolemic rats. Sci Rep-Uk 2018;8. https://doi.org/10.1038/s41598-017-19013-2.

Kwon WB, Soto JA, Stein HH. Effects of dietary leucine and tryptophan on serotonin metabolism and growth performance of growing pigs. J Anim Sci 2022;100. https://doi.org/10.1093/jas/skab356.

Kwon WB, Touchette KJ, Simongiovanni A, Syriopoulos K, Wessels A, Stein HH. Effects of dietary leucine and tryptophan supplementations on serotonin metabolism and growth performance of growing pigs. Eaap Public 2019a;138:303–4. https://doi.org/10.3920/978-90-8686-891-9_82.

Kwon WB, Touchette KJ, Simongiovanni A, Syriopoulos K, Wessels A, Stein HH. Excess dietary leucine in diets for growing pigs reduces growth performance, biological value of protein, protein retention, and serotonin synthesis. J Anim Sci 2019b;97:4282–92. https://doi.org/10.1093/jas/skz259.

Laurent G, German NJ, Saha AK, de Boer VCJ, Davies M, Koves TR, Dephoure N, Fischer F, Boanca G, Vaitheesvaran B, et al. SIRT4 coordinates the balance between lipid synthesis and catabolism by repressing malonyl CoA decarboxylase. Mol Cell 2013;50:686–98. https://doi.org/10.1016/j.molcel.2013.05.012.

Le Bacquer O, Petroulakis E, Paglialunga S, Poulin F, Richard D, Cianflone K, Sonenberg N. Elevated sensitivity to diet-induced obesity and insulin resistance in mice lacking 4E-BP1 and 4E-BP2. J Clin Invest 2007;117:387–96. https://doi.org/10.1172/Jci29528.

Lefterova MI, Haakonsson AK, Lazar MA, Mandrup S. PPARgamma and the global map of adipogenesis and beyond. Trends Endocrinol Metabol 2014;25:293–302. https://doi.org/10.1016/j.tem.2014.04.001.

Li HL, Xu MJ, Lee J, He CY, Xie ZL. Leucine supplementation increases SIRT1 expression and prevents mitochondrial dysfunction and metabolic disorders in high-fat diet-induced obese mice. Am J Physiol-Endoc M 2012;303:E1234–44. https://doi.org/10.1152/ajpendo.00198.2012.

Li HX, Qiang J, Song CY, Xu P. Acanthopanax senticosus promotes survival of Tilapia infected with Streptococcus iniae by regulating the PI3K/AKT and fatty acid metabolism signaling pathway. Front Physiol 2021;12:699247. https://doi.org/10.3389/fphys.2021.699247.

Liu R, Li H, Fan W, Jin Q, Chao T, Wu Y, Huang J, Hao L, Yang X. Leucine supplementation differently modulates branched-chain amino acid catabolism, mitochondrial function and metabolic profiles at the different stage of insulin resistance in rats on high-fat diet. Nutrients 2017;9. https://doi.org/10.3390/nu9060565.

Lopez-Farre AJ, Sacristan D, Zamorano-Leon JJ, San-Martin N, Macaya C. Inhibition of Acyl-CoA cholesterol acyltransferase by F12511 (Eflucimibe): could it be a new antiatherosclerotic therapeutic. Cardiovasc Ther 2008;26:65–74. https://doi.org/10.1111/j.1527-3466.2007.00030.x.

Ma QQ, Zhou XB, Hu LL, Chen JY, Zhu JL, Shan AS. Leucine and isoleucine have similar effects on reducing lipid accumulation, improving insulin sensitivity and increasing the browning of WAT in high-fat diet-induced obese mice. Food Funct 2020;11:2279–90. https://doi.org/10.1039/c9fo03084k.

Manders RJ, Praet SF, Meex RC, Koopman R, de Roos AL, Wagenmakers AJ, Saris WH, van Loon LJ. Protein hydrolysate/leucine co-ingestion reduces the prevalence of hyperglycemia in type 2 diabetic patients. Diabetes Care 2006;29:2721–2. https://doi.org/10.2337/dc06-1424.

Mao Z, Zhang WZ. Role of mTOR in glucose and lipid metabolism. Int J Mol Sci 2018;19. https://doi.org/10.3390/ijms19072043.

Martin SK, Fitter S, Dutta AK, Matthews MP, Walkley CR, Hall MN, Ruegg MA, Gronthos S, Zannettino AC. Brief report: the differential roles of mTORC1 and mTORC2 in mesenchymal stem cell differentiation. Stem Cell 2015;33:1359–65. https://doi.org/10.1002/stem.1931.

Mauras N, O'Brien KO, Welch S, Rini A, Helgeson K, Vieira NE, Yergey AL. Insulin-like growth factor I and growth hormone (GH) treatment in GH-deficient humans: differential effects on protein, glucose, lipid, and calcium metabolism. J Clin Endocrinol Metab 2000;85:1686–94. https://doi.org/10.1210/jc.85.4.1686.

Ministry of Agriculture of the People's Republic of China. Determination of calcium, sodium, phosphorus, magnesium, potassium, iron, zinc, copper, manganese, cobalt and molybdenum in feeds-atomic emission spectrometry (NY/T 3318-2018). Beijing, China: China Agriculture Press; 2018.

Muoio DM, Newgard CB. Metabolism - a is for adipokine. Nature 2005;436:337–8. https://doi.org/10.1038/436337a.

Nasrin N, Wu XP, Fortier E, Feng YJ, Bare OC, Chen SM, Ren XL, Wu ZD, Streeper RS, Bordone L. SIRT4 regulates fatty acid oxidation and mitochondrial gene expression in liver and muscle cells. J Biol Chem 2010;285:31995–2002. https://doi.org/10.1074/jbc.M110.124164.

Niu Q, Li P, Hao S, Zhang Y, Kim SW, Li H, Ma X, Gao S, He L, Wu W, et al. Dynamic distribution of the gut microbiota and the relationship with apparent crude fiber digestibility and growth stages in pigs. Sci Rep 2015;5:9938. https://doi.org/10.1038/srep09938.

NRC (National Research Council). Nutrient requirements of swine. 11th ed. Washington (DC): National Academies Press; 2012.

Pan SF, Zhang L, Liu Z, Xing H. Myostatin suppresses adipogenic differentiation and lipid accumulation by activating crosstalk between ERK1/2 and PKA signaling pathways in porcine subcutaneous preadipocytes. J Anim Sci 2021;99. https://doi.org/10.1093/jas/skab287.

Roh C, Han JR, Tzatsos A, Kandror KV. Nutrient-sensing mTOR-mediated pathway regulates leptin production in isolated rat adipocytes. Am J Physiol-Endoc M 2003;284:E322–30. https://doi.org/10.1152/ajpendo.00230.2002.

Rosewarne CP, Cheung JL, Smith WJ, Evans PN, Tomkins NW, Denman SE, P OC, Morrison M. Draft genome sequence of Treponema sp. strain JC4, a novel spirochete isolated from the bovine rumen. J Bacteriol 2012;194:4130. https://doi.org/10.1128/JB.00754-12.

Salles J, Chanet A, Berry A, Giraudet C, Patrac V, Domingues-Faria C, Rocher C, Guillet C, Denis P, Pouyet C, et al. Fast digestive, leucine-rich, soluble milk proteins improve muscle protein anabolism, and mitochondrial function in undernourished old rats. Mol Nutr Food Res 2017;61. https://doi.org/10.1002/mnfr.201700287.

Sehayek E, Ono JG, Duncan EM, Batta AK, Salen G, Shefer S, Neguyen LB, Yang K, Lipkin M, Breslow JL. Hyodeoxycholic acid efficiently suppresses atherosclerosis formation and plasma cholesterol levels in mice. J Lipid Res 2001;42:1250–6.

Shan TZ, Zhang PP, Jiang QY, Xiong Y, Wang YZ, Kuang SH. Adipocyte-specific deletion of mTOR inhibits adipose tissue development and causes insulin resistance in mice. Diabetologia 2016;59:1995–2004. https://doi.org/10.1007/s00125-016-4006-4.

Staels B, Fonseca VA. Bile Acids and Metabolic Regulation Mechanisms and clinical responses to bile acid sequestration. Diabetes Care 2009;32:S237–45. https://doi.org/10.2337/dc09-S355.

Staley C, Weingarden AR, Khoruts A, Sadowsky MJ. Interaction of gut microbiota with bile acid metabolism and its influence on disease states. Appl Microbiol Biotechnol 2017;101:47–64. https://doi.org/10.1007/s00253-016-8006-6.

Sun Y, Wu Z, Li W, Zhang C, Sun K, Ji Y, Wang B, Jiao N, He B, Wang W, et al. Dietary L-leucine supplementation enhances intestinal development in suckling piglets. Amino Acids 2015;47:1517–25. https://doi.org/10.1007/s00726-015-1985-2.

Tong L. Acetyl-coenzyme A carboxylase: crucial metabolic enzyme and attractive target for drug discovery. Cell Mol Life Sci 2005;62:1784–803. https://doi.org/10.1007/s00018-005-5121-4.

Torres-Pitarch A, Gardiner GE, Cormican P, Rea M, Crispie F, O'Doherty JV, Cozannet P, Ryan T, Lawlor PG. Effect of cereal soaking and carbohydrase supplementation on growth, nutrient digestibility and intestinal microbiota in liquid-fed grow-finishing pigs. Sci Rep-Uk 2020;10. https://doi.org/10.1038/s41598-020-57668-6.

Valeriano VD, Balolong MP, Kang DK. Probiotic roles of Lactobacillus sp. in swine: insights from gut microbiota. J Appl Microbiol 2017;122:554–67. https://doi.org/10.1111/jam.13364.

Vigors S, Sweeney T, O'Shea CJ, Kelly AK, O'Doherty JV. Pigs that are divergent in feed efficiency, differ in intestinal enzyme and nutrient transporter gene expression, nutrient digestibility and microbial activity. Animal 2016;10:1848–55. https://doi.org/10.1017/S1751731116000847.

Wallenius V, Wallenius K, Ahren B, Rudling M, Carlsten H, Dickson SL, Ohlsson C, Jansson JO. Interleukin-6-deficient mice develop mature-onset obesity. Nat Med 2002;8:75–9. https://doi.org/10.1038/nm0102-75.

Wang P, Gao J, Ke W, Wang J, Li D, Liu R, Jia Y, Wang X, Chen X, Chen F, et al. Resveratrol reduces obesity in high-fat diet-fed mice via modulating the composition and metabolic function of the gut microbiota. Free Radic Biol Med 2020;156:83–98. https://doi.org/10.1016/j.freeradbiomed.2020.04.013.

Wang XX, Edelstein MH, Gafter U, Qiu L, Luo Y, Dobrinskikh E, Lucia S, Adorini L, D'Agati VD, Levi J, et al. G protein-coupled bile acid receptor TGR5 activation inhibits kidney disease in obesity and diabetes. J Am Soc Nephrol 2016;27:1362–78. https://doi.org/10.1681/ASN.2014121271.

Wessels AG, Kluge H, Hirche F, Kiowski A, Schutkowski A, Corrent E, Bartelt J, Konig B, Stangl GI. High leucine diets stimulate cerebral branched-chain amino acid degradation and modify serotonin and ketone body concentrations in a pig model. PLoS One 2016;11. https://doi.org/10.1371/journal.pone.0150376.

Yanai H, Yoshida H. Beneficial effects of adiponectin on glucose and lipid metabolism and atherosclerotic progression: mechanisms and perspectives. Int J Mol Sci 2019;20. https://doi.org/10.3390/ijms20051190.

Yang H, Huang XC, Fang SM, He MZ, Zhao YZ, Wu ZF, Yang M, Zhang ZY, Chen CY, Huang LS. Unraveling the fecal microbiota and metagenomic functional capacity associated with feed efficiency in pigs. Front Microbiol 2017a;8. https://doi.org/10.3389/fmicb.2017.01555.

Yang TT, Shu T, Liu GL, Mei HF, Zhu XY, Huang X, Zhang LY, Jiang ZZ. Quantitative profiling of 19 bile acids in rat plasma, liver, bile and different intestinal section contents to investigate bile acid homeostasis and the application of temporal variation of endogenous bile acids. J Steroid Biochem 2017b;172:69–78. https://doi.org/10.1016/j.jsbmb.2017.05.015.

Yeaman SJ. Hormone-sensitive lipase–a multipurpose enzyme in lipid metabolism. Biochim Biophys Acta 1990;1052:128–32. https://doi.org/10.1016/0167-4889(90)90067-n.

Yeaman SJ. Hormone-sensitive lipase - new roles for an old enzyme. Biochem J 2004;379:11–22. https://doi.org/10.1042/bj20031811.

Yuan XW, Han SF, Zhang JW, Xu JY, Qin LQ. Leucine supplementation improves leptin sensitivity in high-fat diet fed rats. Food Nutr Res 2015;59:27373. https://doi.org/10.3402/fnr.v59.27373.

Zambad SP, Tuli D, Mathur A, Ghalsasi SA, Chaudhary AR, Deshpande S, Gupta RC, Chauthaiwale V, Dutt C. TRC210258, a novel TGR5 agonist, reduces glycemic and dyslipidemic cardiovascular risk in animal models of diabesity. Diabetes Metab Syndr Obes 2013;7:1–14. https://doi.org/10.2147/DMSO.S50209.

Zhang HH, Huang J, Duvel K, Boback B, Wu S, Squillace RM, Wu CL, Manning BD. Insulin stimulates adipogenesis through the Akt-TSC2-mTORC1 pathway. PLoS One 2009;4:e6189. https://doi.org/10.1371/journal.pone.0006189.

Zhang YY, Guo KY, LeBlanc RE, Loh D, Schwartz GJ, Yu YH. Increasing dietary leucine intake reduces diet-induced obesity and improves glucose and cholesterol metabolism in mice via multimechanisms. Diabetes 2007;56:1647–54. https://doi.org/10.2337/db07-0123.

Zhao L, Ma P, Peng Y, Wang M, Peng C, Zhang Y, Li X. Amelioration of hyperglycaemia and hyperlipidaemia by adjusting the interplay between gut microbiota and bile acid metabolism: radix Scutellariae as a case. Phytomedicine 2021;83:153477. https://doi.org/10.1016/j.phymed.2021.153477.

Zimmermann R, Strauss JG, Haemmerle G, Schoiswohl G, Birner-Gruenberger R, Riederer M, Lass A, Neuberger G, Eisenhaber F, Hermetter A, et al. Fat mobilization in adipose tissue is promoted by adipose triglyceride lipase. Science 2004;306:1383–6. https://doi.org/10.1126/science.1100747.